Image Guided Stereotaxic

Surgery System

Author

NAMRA AFZAL

NUST2015-MS-BME-00000118246

Supervisor

DR. MUHAMMAD NABEEL ANWAR

DEPARTMENTOF BIOMEDICAL ENGINEERING AND SCIENCES

SCHOOL OF MECHANICAL & MANUFACTURING ENGINEERING

NATIONAL UNIVERSITY OF SCIENCES AND TECHNOLOGY

ISLAMABAD, PAKISTAN.

JANUARY, 2018

Image Guided Stereotaxic Surgery System

Author

NAMRA AFZAL

Registration Number

NUST2015-MSBME-00000118246

A thesis submitted in partial fulfillment of the requirements for the degree of

MS Biomedical Engineering

Thesis Supervisor:

Dr. Muhammad Nabeel Anwar.

Thesis Supervisor's Signature: ___________________________________

DEPARTMENT OF BIOMEDICAL ENGINEERING AND SCIENCES

SCHOOL OF MECHANICAL & MANUFACTURING ENGINEERING

NATIONAL UNIVERSITY OF SCIENCES AND TECHNOLOGY,

ISLAMABAD, PAKISTAN.

JANUARY, 2018

Thesis Acceptance Certificate

I certified that final copy of MS Thesis written by NS Namra Afzal, (Registration No. NUST2015-MSBME-00000118246), of SMME (School) has been vetted by undersigned, found complete in all respects as per NUST Statutes /Regulations, is free of plagiarism, errors, and mistakes and is accepted as partial fulfillment for award of MS/MPhil Degree. It is further certified that necessary amendments as pointed out by GEC members of the scholar have also been incorporated in the said thesis.

Signature: ________________________________

Name of Supervisor: Dr. Muhmmad Nabeel Anwar

Date: ________________

Signature (HOD): ____________________________

Date: ________________

Signature (Principal): __________________________

Date: ________________

Certificate of Approval (TH-4)

Declaration

I certify that this research work titled "*Image Guided Stereotaxic Surgery System"* is my own work. The work has not been presented elsewhere for assessment. The material that has been used from other sources it has been properly acknowledged / referred.

Signature of Student

NAMRA AFZAL

NUST2015-MSBME-00000118246F

Plagiarism Certificate (Turnitin Report)

This thesis has been checked for Plagiarism. Turnitin report endorsed by Supervisor is attached.

Signature of Student

NAMRA AFZAL

NUST2015-MSBME-00000118246F

Signature of Supervisor

Copyright Statement

Acknowledgements

All attributes to Almighty Allah, who led this work to fulfillment and awarding me much more than I deserve. I am profusely thankful to my beloved parents who raised me when I was not capable of walking and continued to support me in every field of my life.

I would like to express special thanks to my supervisor Dr. Muhammad Nabeel Anwar for his help throughout my thesis. Not only as a Supervisor & Head of department, but also as a Mentor. He always motivated and inspired through the thick and thin of my tenure at NUST.I express my deepest gratitude to him for his influence on inspiring me and providing me the directions throughout in this research. Thanks to him for giving me a slot to work in the domain of Image processing by guiding me throughout my entire thesis time span. Without his help I wouldn't have been able to complete my thesis.

I am deeply indebted to my GEC members for their valuable guidance and suggestions especially Dr. Syed Irtiza Ali Shah for his tremendous support and cooperation. Each time I got stuck in something, he came up with the solution. A special thanks to Dr. Umer Ansari for his technical support & Dr. Adeeb Shehzad for his timely inputs and suggestions in my project.

I would like to thank whole Human Systems Lab in which my seniors (Ahmed, Zaid Ahsan Shah, Aqsa, Atif, Usman, Sidra, Ghina, Kinza, Amnah, Saad) and my Colleagues (Amna Maliha and Azmat) were always there to support me. My appreciation goes to my extraordinary friends and classmates, Zaeem Hadi and Sonia Malik, for patiently listening to my problems and trying to resolve them to the best of their knowledge. Special thanks to my room mates Sumbul Gulzar, Anisa Qasim and Sana Saleem from EME College who not only helped me in technical issues but also supported me emotionally in dealing with stress management.

My deepest, heartiest and sincerest regards to my best friends, Zareen Ahmed (My Mother), Dr.Muhammad Afzal (My Father) and Dr. Adeel Ismail for supporting me in every aspect of my project whether it was emotional or practical. I have no words to express my feelings for you.

Dedicated to my loving parents Mr. & Mrs. Dr. Muhammad Afzal and Dr. Adeel Ismail whose tremendous support and cooperation led me to this wonderful accomplishment.

Abstract

Background: Stereotaxic surgery system is minimally invasive form of surgical procedure which requires lot of precision and accuracy especially for invasive neural surgery in order to prevent maximum neurons in brain to be damaged

Objective: Purpose of the thesis is to develop image-based guidance system for stereotaxic cage with ability to track the location of needle or drill on target brain region.

Methodology: Stereotaxic grid system in real world was developed by using NI LabVIEW Vision software. Image acquisition was done using NI LabVIEW Acquisition. In NI Vision Assistant, image processing was done along with mapping from pixel to real world using image calibration. In pre-processing, color plane extraction and thresholding were done. In Perspective Grid Calibration; point of origin, spacing & coordinates were defined for both x and y axis in real world. OpenCV was used for real time drill tracking. For real time motion tracking, mean shift algorithm and red particle analysis were used. After doing histogram and back projection calculation, low saturation points were removed and mean shift algorithm was used for drill tracking. For red particle analysis several steps like calculation of likelihood N4 neighborhood, confidence interval for red color, state of next model estimation, window was set to be auto size, maximum number of particles to be chosen were 1000, vector dynamics & likelihood for each particle was calculated.

Results: Real time drill motion tracking & calibration in real world was done for image guided Stereotaxic Surgery System. Drill bit of 2.35mm diameter was tracked all the way long. Measurements of position, distance & angle in real world were acquired

Conclusion: Mean of distance calculation was 10.147 mm & standard deviation was 0.189 mm. Average inspection time for the whole process was 0.94ms.

Keywords: Stereotaxic Surgery, mean shift tracking, Image Calibration, Red Particle Filter Tracking, Histogram Equalization, Histogram Normalization.

Table of Contents

List of Figures

List of Tables

List of Equations

Chapter 1 INTRODUCTION

Stereotaxic surgery is a surgical procedure in which a brain tumor is removed with aid of image navigation.

Stereotaxic surgery device is used to do minimum invasive surgery. It locates small parts in body via any three-dimensional coordinate system which helps to perform surgical procedures within the body. During surgery, after fixing the head of the patient and sensor arm, the translation of the position of the tip of the sensor arm onto the computed tomography images was showed on a screen was done by taking samples of the standard points. It involves pre-operative, intra-operative as well as monitoring imaging system. Stereotaxic surgery device consists of stereotaxic cage along with computer guided system.

Computer guided stereotaxic system is used along with preoperative CT images to find the exact location of stereotaxic needle inside the body. For the computer guided surgery, preoperative CT or MRI data is combined with three-dimensional intraoperative navigation systems for better analysis of the tissues within the body. This method is done for removing tumors in critical location. We need stereotaxic device to be very precise and accurate especially for invasive neural surgery in order to prevent maximum neurons in brain to be damaged.

In stereotaxic cage after fixing the head of patient via rods on ar, open neural surgery is done along with the positional data translation of the tip of stereotaxic needle. It is done using computer guided system using both pre-operative and intra-operative images data.

In order to achieve greater accuracy, brain atlas can also be used for mapping the brain regions while performing invasive neural surgery. By using interactive software, we can set target in the brain and exact position of surgical tool can be calculated in order to reach the exact location for the desired surgical procedure. By using such real time intra operative and interactive image-guided navigation system, brain surgery will become easy with minimum damage of neurons.

6.1 Imaging Systems for Stereotaxic Surgery

For Stereotaxic Surgery we need two types of image processing systems along real time monitoring system.

1.1.1 Intra operative Imaging system

A system for image-guided visualization stereotactic is required for finding direction in tumor surgery along with frameless stereotaxic navigation technology for video processing which allows the visualization in real-time for medical imaging as a video overlay during the actual surgical procedure. Intra-operative simulated computer generated anatomical structures need to be displayed. This result in navigation for surgical assistance without limiting the intuition of the surgeon based on the continuous observation of the functional field.

1.1.2 Pre- operative system

For pre-operative system we need any imaging modality to be used in order to locate the brain region to be targeted for electrode placement, drilling during craniotomy or tumor removal. Such system is then combined with intraoperative navigation within the body. The term used for it is called computer aided surgery systems. Such systems are used in artificial robots as well for surgical assistance.

1.1.3 Monitoring imaging systems

Such systems are used in robotic surgical systems in order to know exactly where drill is going and to identify its location. Such systems need to be tracked especially in remote robotic surgery or in automated surgery system.

6.2 Types of Stereotaxic Surgery Frame

1.1.4 Stereotaxic Frame

Stereotaxic frame is normally used for human head. Its size is varied according to human head. Surgical tools are attached with it for operating.

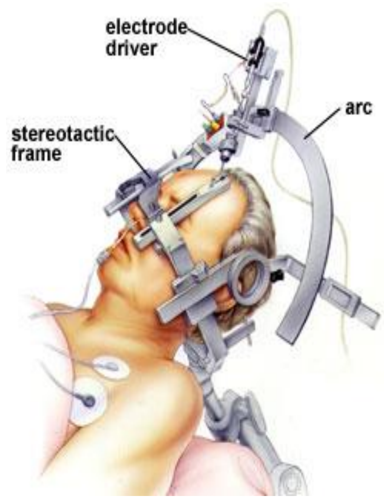

Figure 1: Stereotaxic Frame

1.1.5 Free standing Manipulator

Such free-standing manipulator is used for animals like rats, rodents & rabbits with rods to hold their head in place. Rods are used to tighten their heads via their ears. If free standing manipulator is moveable it can be used for different animal head size

Figure 2: Free standing Manipulator

Such device can be converted onto a

- Adult stereotaxic surgery frame
- Free standing manipulator for animals of varying head size.

The frame of head-stabilizing device allows head positioning to be fixed

- to attain accurate vertical &
- horizontal positions

This flexibility also allows the system to accommodate range of animal head sizes.

6.3 Applications of stereotaxic Surgery

- It is used to ease precise path for moving surgical device through the brain and for safe removal of abnormal tissue without brain shift with normal undamaged healthy brain.
- Can be used to repair fracture, repair blood vessels, to treat brain conditions like epilepsy, hematoma, drug delivery
- Such systems from imaging modality interventions in real time displays surgeons where their tools are in brain of patient.
- Used for Preliminary method for craniotomy
- DBS (Deep Brain stimulation)
- Stereotaxic Biopsy
- Gamma knife radiosurgery (noninvasive)
- Tumor detection
- Accurately locate brain region
- Stereotaxic device need to be very precise especially for invasive neural surgery in order to prevent maximum neurons in brain to be damaged
- Tumor e.g., gliomas
- Can be used to repair fracture, meninges, repair blood vessels, to treat brain conditions like epilepsy, hematoma, drug delivery

6.4 Objective of study

‘‘Development of image-based system for stereotaxic surgery’’

6.5 Thesis layout

Chapter 1 contains introduction which contains significance, problem statement and objectives. This chapter also contains types and application of stereotaxic Surgery System along with details of Stereotaxic imaging systems.

Chapter 2 deals with Literature Review, history, challenges and research gaps in detail and also include discussions related to stereotaxic surgery including catheter position in US patents device, 3D MRI based system, remote robotic surgery etc.

Chapter 3 includes methodology in detail. Module 1 contains Drill tracking using mean shift algorithm. Module 2 contains drill tracking using red particle filter. Module 3 contains calibration and real-world mapping using LabVIEW.

Chapter 4 includes Results in detail. It includes all the graphs, figures, and tables of results in both OpenCV and LabVIEW vision. It also includes discussion of results as well. Problems in each module is are also discussed here.

Chapter 5 includes conclusion of all the modules and future works which can be done in future research.

Chapter 2 Literature Review

A system was developed as an assistant for computed tomography guided stereotaxic brain surgery. It consists of a multi joint three-dimensional sensor arm and a microcomputer which shows the location of the tip of sensor arm on the preoperative computed tomography images. Pre-operatively computed tomography scan is completed using three pointers positioned on ears. By this method, positional data from preoperative computed tomography scan can be directly moved into the stereotaxic surgical field. The exclusive feature of this system is presentation of computed tomography guided stereotaxic into predictable open neurosurgery.

The term computer aided surgery is now basically used for an intraoperative neuro navigation inside the body merging a three-dimensional digitizer with preoperative imaging modality. This technique has become essential in neurosurgery for the tumor removal of deep-rooted, critically situated intracranial and vascular malformations. Computer Aided Systems are used in Surgeries like ENT for the paranasal sinuses and in orthopedic surgery for setting of pedicle screws for high targeting accuracy. And still such methods are used in surgical procedures in growing number. Today infrared optical three-dimensional digitizers are being used but innovative, small localizers using electromagnetic spatial digitizing are capable, too.

It included historical review of papers regarding the usage of deep brain stimulation to the thalamus region to cure the symptoms of Tourette syndrome. Citation has been done using seminal paper of Hassler and Dieckmann. The translation of seminal paper of stereotaxic surgery is done and discussed in English language. [1]

Data of craniometric and stereotaxic surgery of rats of varying gender and weights were compared. It was found that stereotaxic brain atlas can be used with data of rats of different gender given that the weights of the rats relate to those used in the reference atlas. If rats of varying weights are used, more precision can be attained if bregma is taken as the reference point for surgery with rostral structures and the intraural line to work with caudal structures.[2]

An ultrasound imaging system includes an ultra sound transducer and an image processing part for 3-D ultrasound image acquisition of the patient's body, it also includes a catheter for diagnostic or investigative intervention in the patient's body. The catheter adjusts according to the customized instruments essential to perform its task, ultrasound receivers which are three in number are fixed at a specific distance from one another on the catheter's tip and it can detect the arrival of signals of the transducer. The calculated distance between the ultrasound transducer and the receivers can be found from the signals using their transit time. The receivers are restricted in space. Localization permits particular selection of the plane from the 3-D ultrasound data which holds all the three receivers of the catheter. The catheter's tip can thus be tracked automatically and presented on the monitor in real time without manual movement of ultrasound transducer [3]

In this paper, it is described that how a Unimation Puma 200 robot, appropriately interfaced with a computed tomography scanner and a probe guide connected to one of its end. It can be used for computed tomography guided brain surgeries. Once the target is set on the computed tomography preoperative image, the robot moves to a position in such manner that the end of the probe points out the target region. This results in a faster procedure as compared to the manually adjustable stereotaxic frame. As mentioned in this paper that the improved precision can be achieved through proper calibration of the device.[4]

A system developed for identifying a probe's tip position which is positioned inside an object on scanned and cross-sectional images of the object. The reference points are included in the object. The images of the object contain reference images relative to the previous defined reference points. An array for getting radiation produced by probe and from reference points is converted to digital form by a 3-D digitizer to measure the position of the probe's tip corresponding to the object's reference points. A software translates the location of probe's tip into a coordinate system relative to the coordinate system of the cross-sectional images. A stereotaxic image guided system chooses the image of the object nearest to the measured position of the probe's tip. It displays the carefully chosen image and a cursor for representing the position of the probe's tip on the respective images.[5]

In past few years there has been a significant development in the quality of ultrasound imaging. The integration of three-dimensional ultrasound combined with neuro navigation technology has formed an effective and reasonable tool for intra-operative imaging in neuro surgery. The technical background and a summary of the extensive range of different applications are discussed in this review. This technology has been used to improve removal of tumors in brain surgery. It has also been beneficial in other procedures such as operations for syringomyelia, medulla tumors, skull based tumors, aneurysms, AVMs, cavernous hemangiomas, and endoscopy direction.[6]

Stereotaxic neuro surgery needs 3-D localization of lesions for biopsy or treatment. The objective of this paper is to define the approaches used in varying imaging modalities such as X-ray, tele-radiography, digital subtracted angiography, computerized tomography, and nuclear magnetic resonance imaging. [7]

For determined target localization methods are distinguished from those helping to define the target measurements necessary for treatment preparation and planning. The precision and problems of these methods are highlighted. The explicit procedure developed in Lille is defined by example. Structural aspects are needed to ensure the efficiency of the procedure i.e. from imaging to treatment, are also discussed. [8]

According to US patent methods are described to analyze internal tissues and US patents can be used for better accuracy as it combined magnetic resonance coil system with magnetic resonance imaging system which makes it easy to locate exact position for catheter position in body. These methods can be followed for determining position of device within brain.[9].According to US Patent by using cross sectional images which are scanned we can also locate position of probe or device. The object image has specific reference points accordingly. Probe emits radiation which is received by receiver which is mapped according to coordinates for position measurement after being digitized by 3D digitizer. [10] Program reads and translates these coordinates for mapping. In stereotaxic imaging system image of nearby tissue as well as position of device is shown simultaneously.

For improving further position accuracy Puma 200 robot was introduced for better position accuracy of stereotactic surgery. This robot is interfaced with CT scan and for navigation a probe guide is also attached. Hence, it combined navigation along with CT imaging. It can also be used for neuro navigation. Once target is defined, it achieves its goal via CT guide which locates the target. It is quite fast and very precise method to be used.[4]

The main idea of grid system was taken from [11] in which grid coordinates were overlapped with previously taken MRI images to develop brain atlas. However, it was customized and used photo shop instead of doing image processing coding. Secondly it dealt with only brain atlas development not with intraoperative 3D systems.

Stereotaxic brain atlas of the mouse is vital in research for targeting specific brain regions during surgical operations. The efficiency of stereotaxic surgery is dependent on precise brain regions mapping relative to the markers on the head. Throughout postnatal growth in the mouse, quick changes related to growth in the brain happens simultaneously along with growth of bony plates at the cranial sutures. Mature and developed mouse brain atlas cannot be used to exactly navigate in developing brains. In this study, 3-D stereotaxic atlases of mouse brains at six postnatal progressive stages and two mature adult mouse brain were established, by means of DTI and micro CT.

Presently, extensively used stereotaxic brain atlas of the mouse brain are created on study of tissue but the anatomical dependability of ex vivo atlases to in vivo mouse brains has not been estimated before. The reason for ex vivo tissue misrepresentation due to complex as well as individual changeability in brain. A population averaged in vivo MRI adult mouse brain stereotaxic atlas was developed and a misrepresentation altered diffusion tensor imaging atlas was generated by nonlinearly distorting ex vivo data to the averaged population in vivo atlas. The atlas resources were established and completed through a user interface software with the aim of refining the precision of target brain anatomy during stereotaxic surgery in developing and mature as well as developed mouse brain.[12]

Using change in impedance difference while drilling this neuro star device is used for stereotaxic surgery. However, image guided software system was not developed in it. A great range of neuroscientific methods with in vivo electrophysiology, two-photon imaging, optogenetics, lesions, and micro dialysis, need access to the brain region through the skull. Preferably, the essential craniotomies could be completed in repeated and automated manner, without damaging the original brain tissue. When drilling through the skull a conventional increase in conductance can be detected when the drill bit passes through the skull. [13]

Architecture for a robotic system along with two applications. One based on homebuilt hardware and other based on commercially available hardware that can repeatedly detect such changes and produce large numbers of accurate craniotomies even in single skull. This technique can be modified to robotically drill in diameter for cranial windows in several millimeters. Such robots will not only be useful for neuroscientists to perform both small and large craniotomies more steadfastly but can also be used to make precisely aligned craniotomies with stereotaxic registration to typical brain atlases which will be problematic to drill manually.[14]

Most of the tumor removal by keeping healthy tissue intact in open cranial surgeries is critical to the scenario for patients with brain cancers. Preoperative magnetic resonance images are normally used for surgical development as well as for intraoperative image-guidance.[15]

Brain shift even at the beginning of stereotaxic brain surgery knowingly compromises the accuracy of neuro navigation, if the warp is not compensated for. Compensation for brain shift during brain surgery is therefore serious for refining the precision of image-guidance and eventually, the precision of surgery. Integrated neurosurgical guidance system that incorporates intraoperative 3-D tracking, acquisition of 3-D ultrasound, stereo-vision, and computational modeling to proficiently create updated magnetic resonance images for neurosurgical navigation was established. The system is applied with real time LabVIEW to provide high accuracy in data acquisition as well as with MATLAB to offer computational ease in data processing and progress of GUI related to computational modeling. In a distinctive patient case, the patient in the OR i.e. operating room is first registered to image data. Rare displacement data extracted from co registered intra-operative ultrasound or stereovision images are used to guide a computational model that is based on merging or consolidation theory. Computed whole brain distortion is then used to produce an updated MRI data for consequent surgical guidance. In this paper, we present the significant modular components of our integrated model based neuro navigation surgical system.[15]

A complete software package called ANALYZE has been established which allows comprehensive investigation and assessment of multidimensional images related to biomedical. ANALYZE can be also be used with three-dimensional imaging modalities created on x-ray computed tomography, radionuclide emission tomography, ultrasound tomography, and magnetic resonance imaging MRI. The ANALYZE suite has integrated features, complimentary tools for fully interactive display, manipulation, and measurement of multidimensional image data. It provides an effective customized prototyping and applications. This paper delivers a general picture of ANALYZE as well as specific details on the method working to develop it, both conceptual and technical. Applications of the software are illustrated.[16]

Interactive system for navigating the surgical tool using at least one imaging modality, such as computed tomography. An automatic arm has base at the first end and a holder that contains surgical device is at another end. A display shows images from the image data of a patient's structural anatomy data. A computer is attached to the display and the automatic arm. The computer tracks the location of the surgical device in physical coordinates after performing a transformation from physical coordinates to the image coordinates and it causes the display to show the position of the surgical device within the image coordinates.[17]

Pedicle bolt insertion method has made revolution in the surgical handling of spinal problems. Navigation based on fluoroscopy X- ray is common and there is danger of continued exposure to X- ray radiations. Systems with lower radiation are usually costly. The location and angle of the drill is clinically significant in fixation of pedicle screw. In this paper, the location and angle of the marker on the drill is determined using techniques based on pattern recognition, by using morphological features, obtained from the input video in real time using CCD camera. After preprocessing a search is then completed on the subsequent video frames to get the exact location and angel of the drill. Animated illustrations, showing the location and angle of the drill instantaneously is then covered on the real time processed video for control and navigation of drill.[18]

Stereotactic surgery can be used via major imaging modalities like Ultrasound, CT, and MRI. Each one of them has its own advantages and disadvantages. CT and MRI are used mainly for preoperative imaging and ultrasound for intra operative imaging. These techniques combined with neuro navigation tools can be used to exactly locate the brain tumor within skull despite the fact of brain shift. In order to increase accuracy technique of US patents to know the position of device in body along with Puma 200 robot technique can be combined to make high frequency, accurate, fast stereotactic device along with detection of tumor location via imaging tools.

Chapter 3 Methodology

6.6 Concept Model

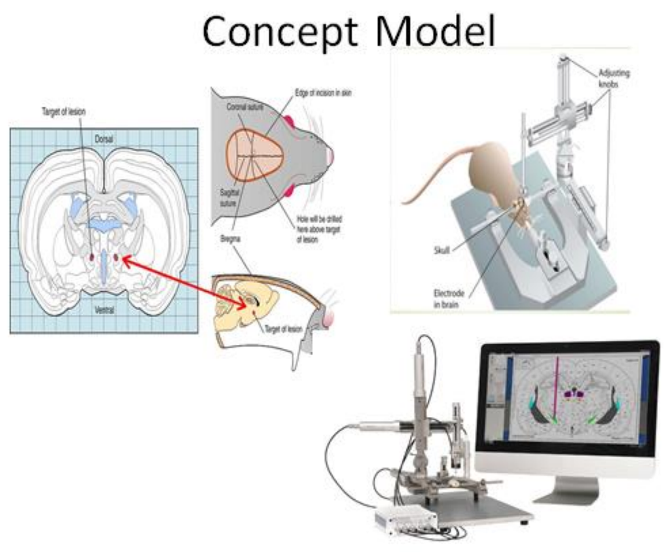

Figure 3: Concept Model contains brain atlas and image guided system along with stereotaxic cage

6.7 Concept model for brain atlas

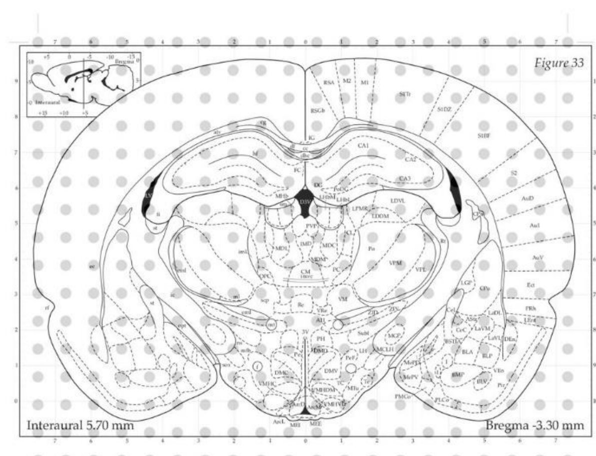

Figure 4: Concept model for brain atlas

6.8 Drill motion tracking using mean shift algorithm in OpenCV

3.1.1 Camera setup

- XYZ stage was setup
- Lead screw-based stage

Advantages of lead screw

Image acquisition setup was added It had precise, accurate and smooth linear motion. Minimum step size of 8.75µm on the z axis

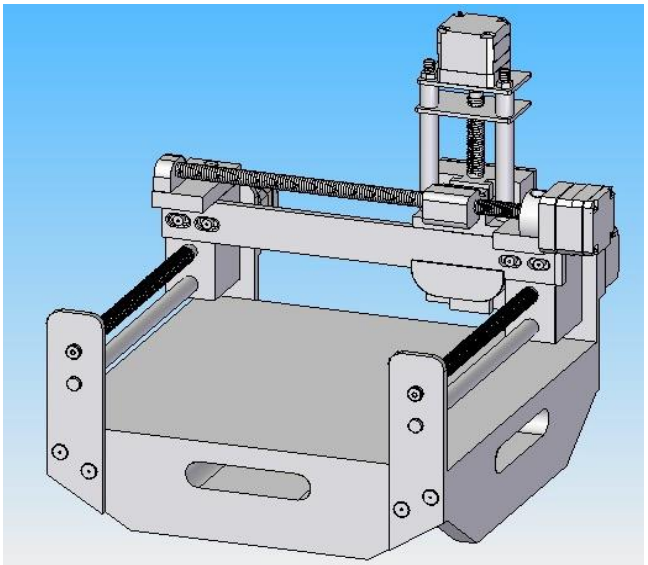

Figure 5: XYZ stage used for linear motion along z axis

3.1.2 Video Acquisition Setup

- XYZ stage was used with white background for better vision
- Distance of drill measured from camera lens was 15 cm
- Height of camera setup was measured to be 11cm
- Diameter of drill (to mimic Marathon Escort dental drill) used was 2.1 mm

Figure 6: Vision acquisition setup with XYZ lead screw stage used for linear motion along z axis

3.1.3 Marathon Escort dental drill

Figure 7: Marathon escort dental drill III

3.1.4 Marathon Escort Dental Drill Specifications

- Diameter of drill bit at tip was 1.96 mm
- Voltage is about 220 to 240 volt
- Micro motor Escort-III
- portable and compact size
- 0 to 35 thousand rpm, less vibration standard carbon brush motor
- less heat generation after hours of operation as it has effective electrical design
- Non-Stage speed dialing system
- Non-stage speed system (it's well designed to output from zero to 35 thousand rpm by using non stage speed system)
- Right / left turning ability
- Standard Bur size is about 2.35 mm
- Also has On/off switch
- Power is 65 watts
- ac power supply 220 to 240 voltage and frequency 50 Hz to 60 Hz

3.1.5 Drill motion tracking flowchart

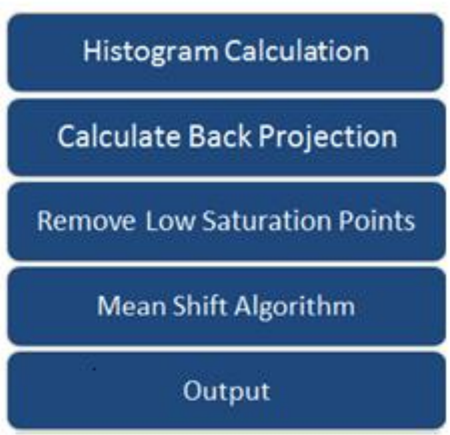

Figure 8: Flow chart of mean shift algorithm Motion tracking of drill bit 1.96 mm

3.3.5.1 Libraries used in OpenCV

Libraries used were of tracking, high GUI, image processing, input output, background segmentation and object detection were used.

3.3.5.2 Take each frame of the video in real time

Video Capture' command was used to get video streaming from TX-5000 USB camera with frame rate of 30 frames per second. Video streaming was in real time. Current frame was taken and whole process was implemented on it using while loop.

3.3.5.3 RGB to HSL conversion

RGB to HSL plane conversion was done because camera does not perceive color as human eye does. For HSV, the range of Hue is 0 to 179, range of Saturation is 0 to 255 and range of Value is 0 to 255. Different software use different scales. So for comparing values in OpenCV with them, it was needed to normalize the ranges. So these ranges were normalized after taking histogram. It was done because camera does not perceive colors as human eyes perceive so for better color extraction and detection, HSL plane is used.

- It takes each frame of the video in real time
- Convert from RGB to HSV color plane
- Calculate histogram
- Normalize histogram
- Thresholding the HSV image for a range of red color
- The red object is extracted i.e. drill bit in video

3.3.5.4 Histogram calculation

Histograms are organized counts of data collected together and managed into a set of predefined number of bins. OpenCV implements the function of calculate Histogram, this function calculates the histogram of a set of arrays which are usually images or image planes. It can work with up to 32 number of dimensions.

HSL(hue, luminance & saturation). It works best with colors in luminance. HSL plane is used because it is near to what human perceive color.

What does this program do?

This program does the following steps:

- It loads an image
- It converts the image into its RGB planes using the split function
- It calculates the histogram of each plane by calling the calculate histogram function

Mat object

The first thing about Mat is that it does not need user to allocate the location of its memory by hand and it releases it as soon as user does not need it. While doing the process there is still an option that most of the functions in OpenCV allot memory location to its output data routinely. In other words, it can be used at all the times as much of the memory as we want to perform the specific task.

Mat is actually a class with two data parts. In the first one is the matrix header which contains the information such as the technique used for storing, the size of the matrix, the position of address at which the matrix is stored, etc. and in second one it contains a pointer pointing to the matrix containing the values of the pixels depending on the method chosen for loading by taking any dimensionality .The size of the matrix header is constant, however the size of the matrix itself can differ from image to image depending on the image and typically is greater by the orders of the magnitude.

3.3.5.5 Histogram equalization

- It is a technique that recovers the contrast in an image, to spread the intensity range.
- From the image the pixels seem gathered around the middle of the available range of intensities. Histogram Equalization stretches out this range.
- This process is also known as stretching which is used to stretch the color intensity range.

3.3.5.6 Calculate back projection

- Back Projection is a method of recording in a histogram model, that how well the pixels of a image fit the distribution of pixels
- Back Projection calculates the histogram model and then used it to find this feature in an image.

Following steps shows how it works:

1. In each pixel of given Image i.e. p(i,j) the data is collected, and the correspondent bin is found location for this specific pixel i.e
2. Histogram model in the correspondent bin is found ($h_{(i,j)}$,$s_{(i,j)}$) and the bin value is read.
3. Normalization of histogram is done to make output visible then the bin value is stored in a new image i.e. Back Projection.
4. After applying the above-mentioned steps, Back Projection image appears in output.
5. The values stored in Back Projection represent the probability in terms of statistics, that a pixel in given image belong to a specific color, based on the histogram model. For example, in given image, the brighter areas are more probable as compared to the darker areas which have less probability. These darker regions belong to sides that have some shadow on it, which in result affect the detection

3.3.5.7 Remove Low Saturation Points

Low saturation points were removed because mean shift algorithm works on maxima values that is the reason low saturation points are removed in order to get high saturation points.

3.3.5.8 Mean shift algorithm

The perception behind the mean shift is quite simple. Consider a set of points which can be a pixel distribution in histogram back projection. a small window which can be circle or rectangle and that window is moved to the maxima area i.e. where maximum pixel are available with higher saturation. As shown in the image below:

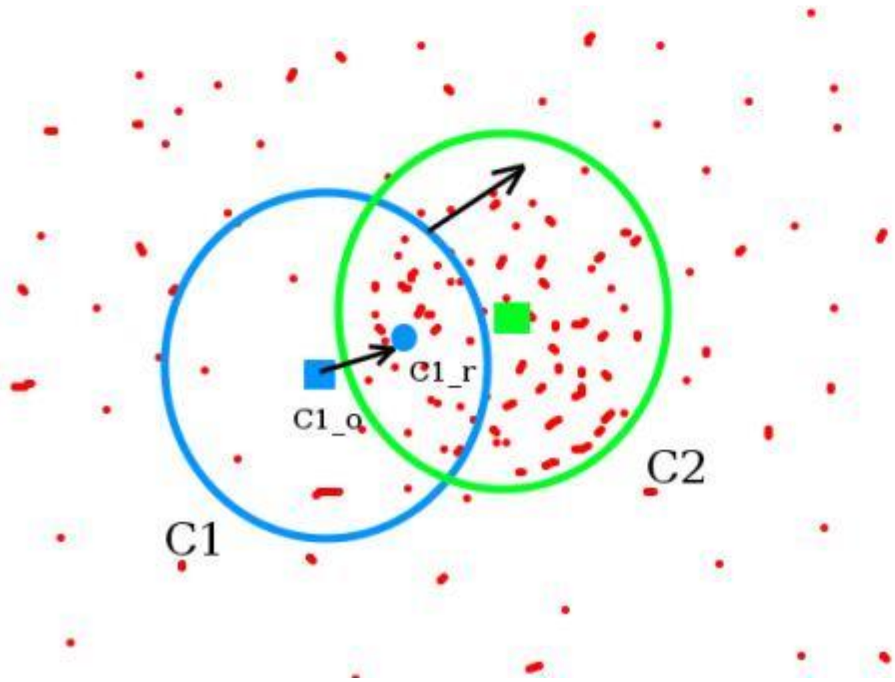

Figure 9: Mean shift algorithm

In this hypothetical example, the original starting window is represented in blue circle with the mentioned name C1. Its initial center is marked in blue rectangle with mentioned name of C1_o. If centroid of the points is found inside that window with mentioned name C1_r represented with small blue circle which is the original centroid of this window. As they don't match. As window is moved in such manner that circle of the new window matches with previously found centroid. Repeatedly, new centroid is found which possibly will not match. So, it is moved again in nonstop iterations such that center of window and its centroid reside on the same location with very small error. So finally, a window with maximum pixel saturation is obtained which is marked with green circle mentioned with name C2.

The histogram back projected given image is passed as well as initial target position. So as the object moves the movement is reflected onto the histogram back projected image. In result, mean shift algorithm moves window to the new position with maximum pixel saturation.

For mean shift in OpenCV, the target needs to be set in order to find its histogram model so that we can back project the target respectively for the mean shift calculation. Initial position of window need to be defined. For calculation of histogram, hue is considered only. To avoid incorrect values due to shadow or low light, values of low light are removed by using **cv.inRange()** function.

3.1.6 Mouse clicking for ROI selection

Callback function was defined in the OpenCV C++ code. That callback function is called each time when the mouse event occurs. That callback function will result in x and y coordinates of the mouse event upon clicking.

It not only gives Value of pixel coordinates, it also gives value of that specific pixel where click is done Secondly, it also allows user to select ROI for moving object which needs to be tracked.

Results

The experimental results show that this method has good presentation in real-time and has satisfactory robustness and positioning accuracy.

3.1.7 Finding Position coordinates on mouse clicking

To know exactly where drill is actually for finding distance traveled by drill pixel coordinates were found it not only gave pixel coordinates upon clicking but also gave value of pixel value in luminance for red its range was from 150 to 172, this is because luminance channel was chosen at that specific point. Maximum value for luminance is 240 and minimum value for is 0 luminance. Following figure shows the results as upon clicking red drill bit values from 150 to 172 were observed. It not only gave luminance value it also gave coordinate values in pixel at that specific point from which it can be checked where exactly drill is in video output.

6.9 Red Particle filter tracking

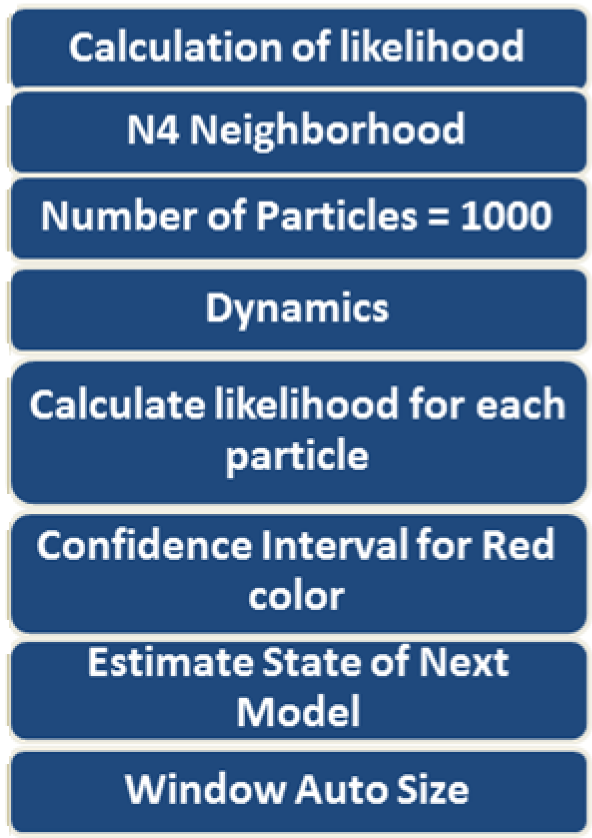

Figure 10: Red particle tracking

- It can cause failure of tracking when the light changes and deformation of the target region occurs.
- The particle filter shows the probability distribution of the given image with a set of weights so that approximation of the state of the next model is done.
- The weight of the particle is measured by the comparison between the under-consideration image and the target image model.

Finding a consistent and robust feature for target is the key of the particle filter tracking algorithm. Presently, color information (i.e. red color was taken other than this Motion information as well as edge features are the mostly used.

The target has good stability which has color distribution and it is not sensitive to the distortion or warp. It can easily be affected by the luminance change and surrounding conditions. To reduce the intrusion of background, the typical color distribution with the value of the weights using kernel window is improved. Secondly, to predict the state use the improved histogram of color. If you use HSL color model then it is better.

Equation 1

distance = sqrt (blue * blue + green * green + (255.0 - red) * (255.0 - red))

In calculating likelihood, if input color is close to red, distance becomes smaller. In here, Blue and green color do not play any role but if you set some target color then track the color.

Equation 2

distance. = sqrt ((target Blue - b) ^2 + (target green - g) ^2 + (target red-r) ^2

Results

Red particle filter analysis takes time i.e. error correction time to reach red drill. It took about average 0.01 seconds to reach red point.

6.10 NI LabVIEW Vision

- LabVIEW stands for Laboratory Virtual Instrument Engineering Workbench.
- VDM (Vision Development Module) and VAS (Vision Acquisition Software)
- Vision and motion IMAQ and IMAQdx
- Vision Express
- Vision Assistant Software
- Vision Acquisition Software

3.1.8 Why LabVIEW?

- Fast
- Image acquisition
- Grid Formation
- Real world mapping was easy
- User friendly customized Vision application could be developed
- The Vision Development Module VDM is designed to develop and organize applications of machine vision.
- It includes functions to acquire images from a number of cameras and process images by enhancing the features, checking the presence of feature, tracing the features, identifying the objects, and calculating the parts.

3.1.9 Actual Grid Size

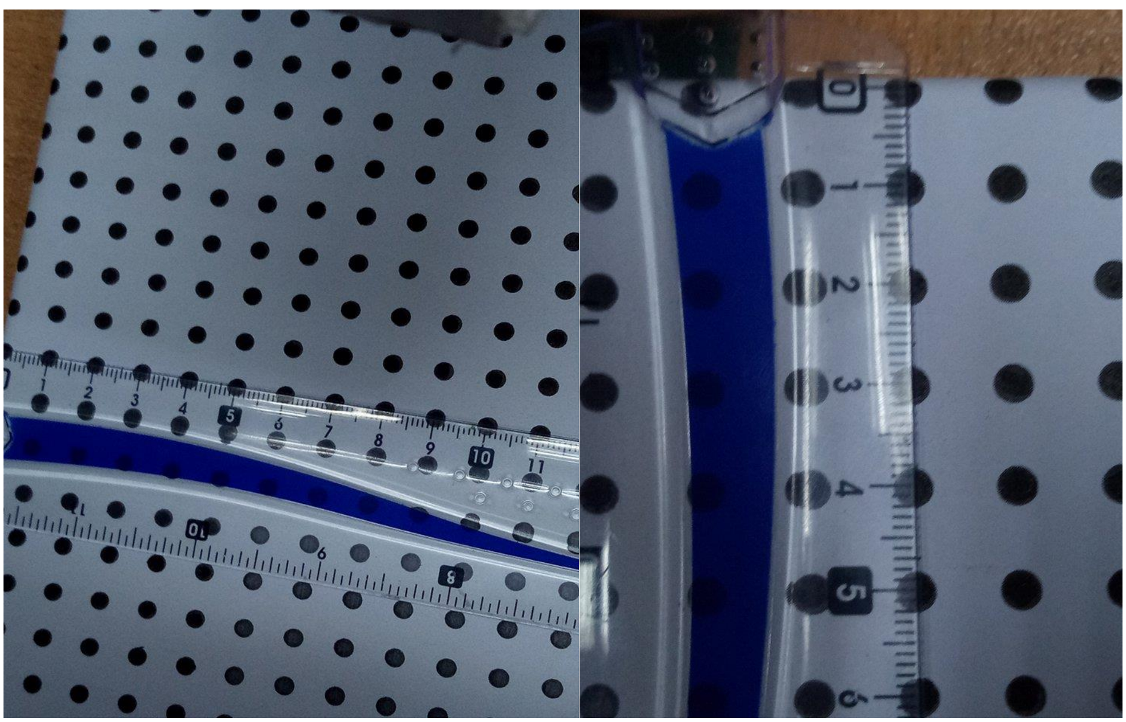

Figure 11: Actual Grid Size

3.1.10 General Design of Vision Application for getting measurement ready image

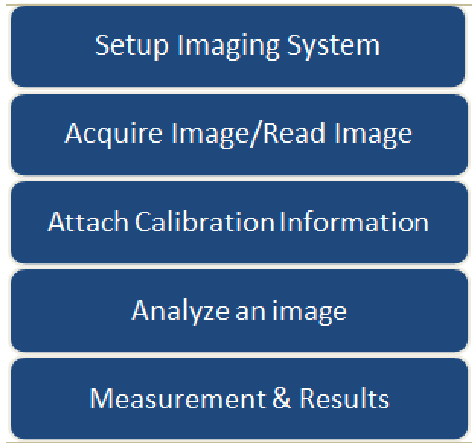

Figure 12: Flow Chart of General Design of Vision Application

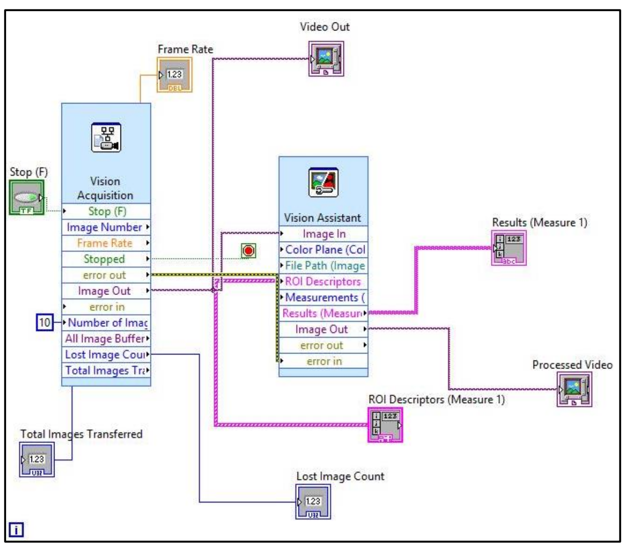

Figure 13: General Design of Vision Application

3.1.11 Vision Acquisition

- USB camera i-tech TX-5000 premium was used
- Inline processing was used with most recent image
- Buffers with 10 image buffers was also used to make sure no image was lost during each process

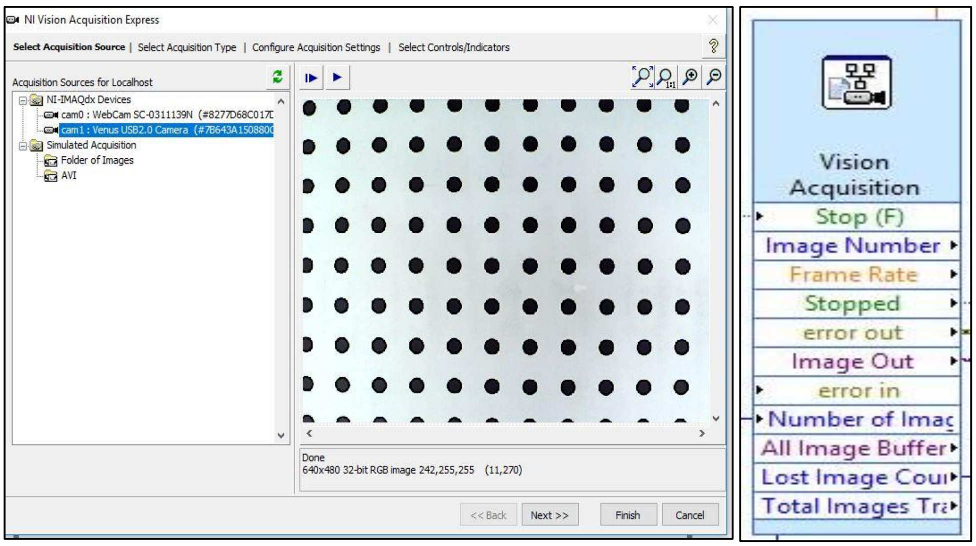

Figure 14: NI Vision Acquisition Express

3.1.12 Continuous acquisition

- Continuous acquisition is used for continuous Image
- Buffers were used to avoid any image to be lost
- Average image processing time must be less than image acquisition time to avoid missing images

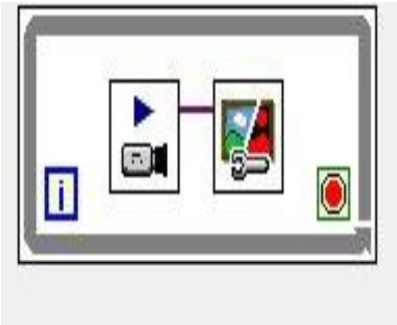

Figure 15: Continuous acquisition

3.1.13 Setup of Image Acquisition

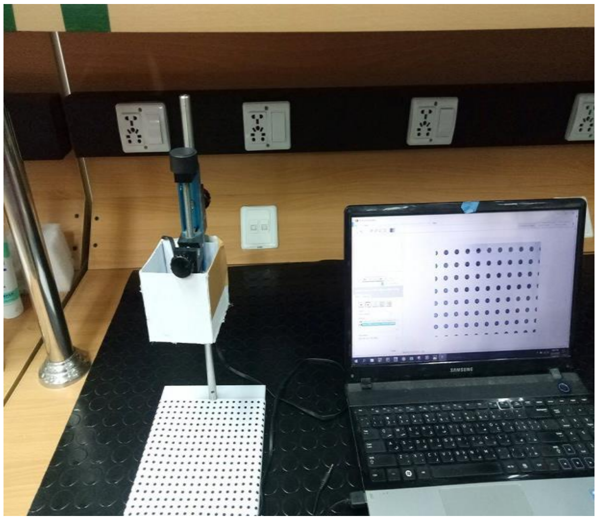

Figure 16: Setup of Image Acquisition

- Camera height was 14 cm
- Manipulator was used for fixing camera
- Base was used as platform for dot grid
- Acquires with resolution 640*480 and 30fps

3.1.14Requirements of Dot grid:

3.5.7.1 Minimum Dot Size

- The actual size of the dot will vary based on the number of pixels of the camera and field of view selected of the camera
- An optimal size is at least 9 pixels (3 x 3), which will ensure the camera will detect the dot accurately and IMAQ Vision will correctly process the dots

3.5.7.2 Minimum Dot Spacing

- The individual dots should be at least 4 pixels apart.
- This will prevent two or more dots from being processed as one dot.

3.5.7.3 Quantity of Dots Consideration

- As the number of dots in the field of view increases, the calibration of the image (in software) becomes better.
- For irregular or curved surfaces, a greater number of dots will insure the contour of the field of view is more accurately represented.

Grid Layout

The dots need to be in vertical and horizontal lines that are perpendicular to each other to make up the grid

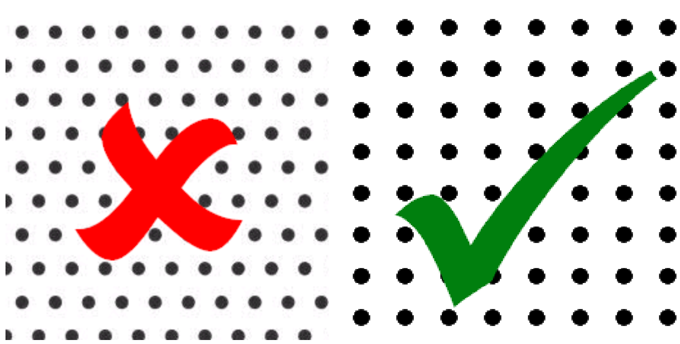

Figure 17: Grid Layout

3.1.15 Vision Assistant

- Vision Assistant is a tool for prototyping and testing image processing applications.
- To prototype an image processing application, build custom algorithms with the Vision Assistant scripting feature. .
- After completing the algorithm, you can test it on other images to make sure it works.
- The algorithm is recorded in a script file, which contains the processing functions and relevant parameters for an algorithm that you prototype in Vision Assistant.
- Can also acquire images single, continuous & in sequence.

3.1.16 Complete Process

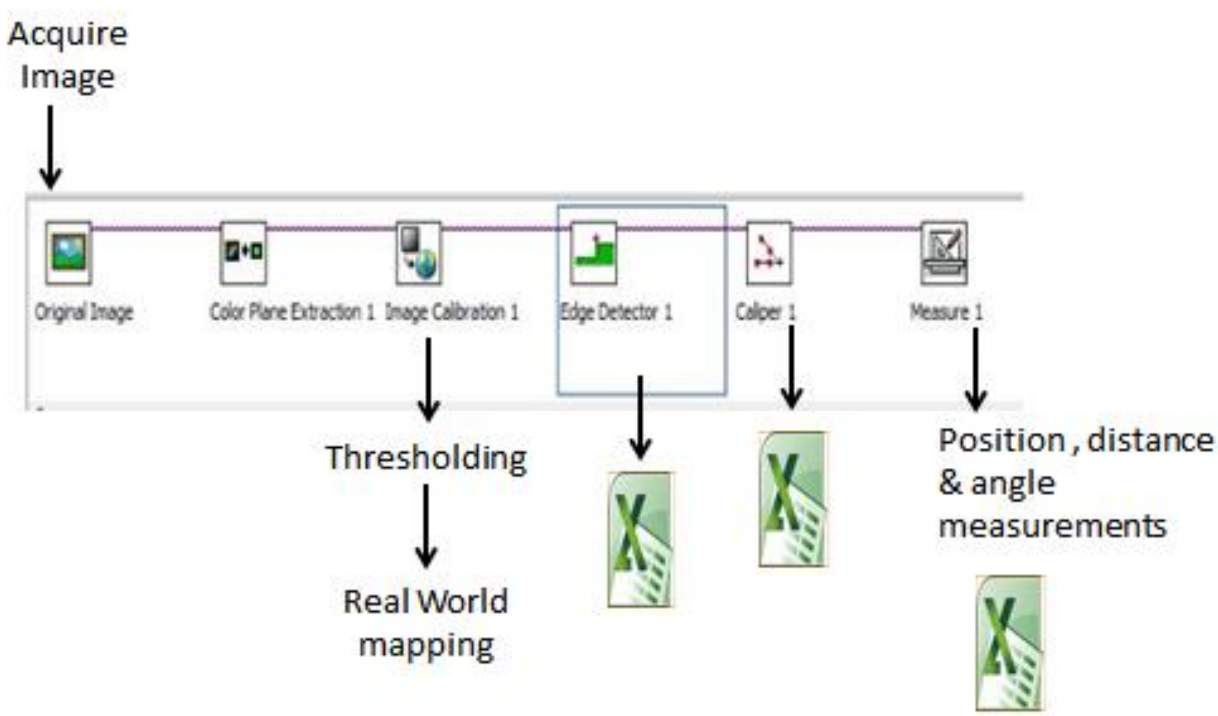

Figure 18: Complete Process

3.1.17 Embedded Code

Using the LabVIEW VI Creation Wizard, I created LabVIEW VI that performs the

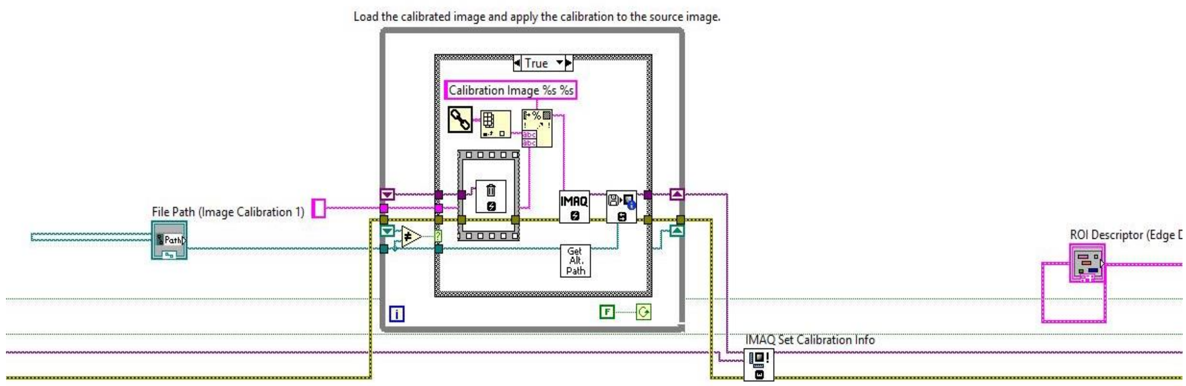

Figure 19: Embedded Code

prototype that was created in Vision.

3.1.18 Steps for Implementation in Vision Assistant

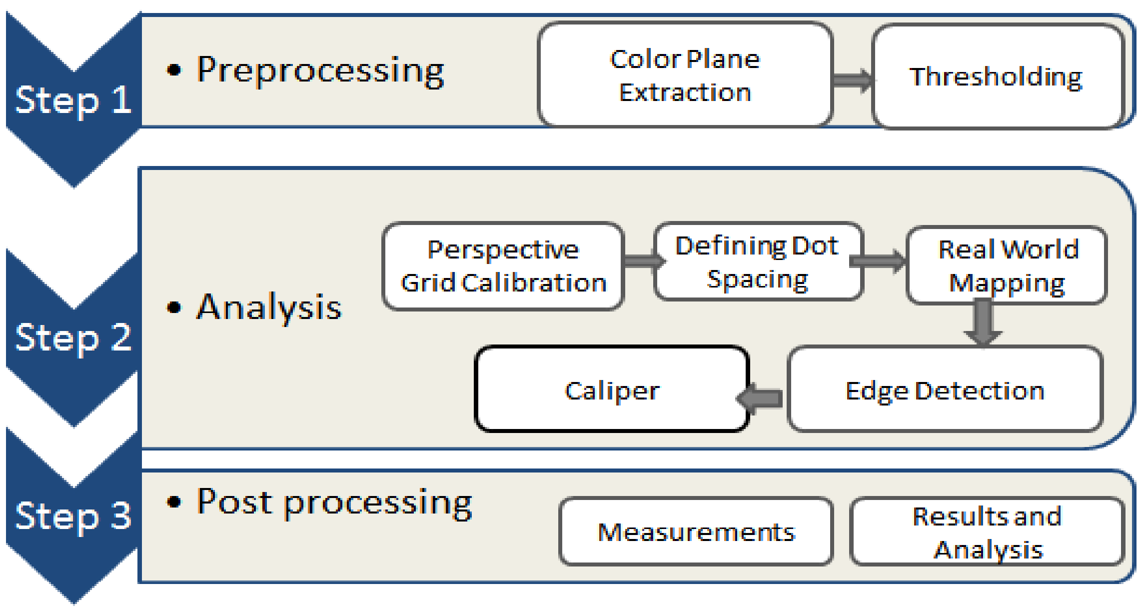

Figure 20: Steps for Implementation in Vision Assistant

3.6.3.1 Step 1 Preprocessing

Color Plane Extraction

- HSL Luminance plane
- Converts image from 32bit to 8bit
- Speeds up the process
- Made thresholding easy

Figure 21: Color Plane Extraction

3.6.3.2 Step 2 Analysis

Image Calibration

- Perspective calibration
- Thresholding
- Real world mapping
- Calibration axis

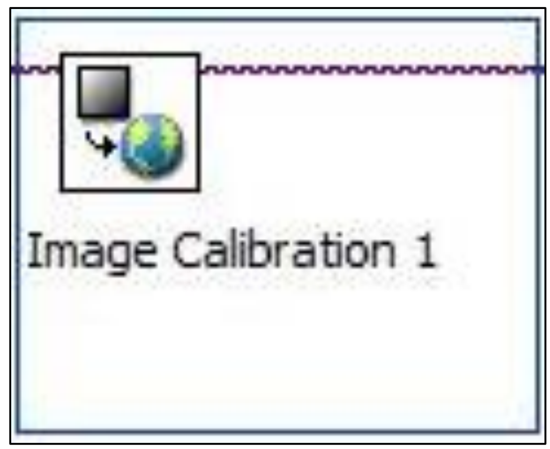

Figure 22: Calibration

Perspective Calibration

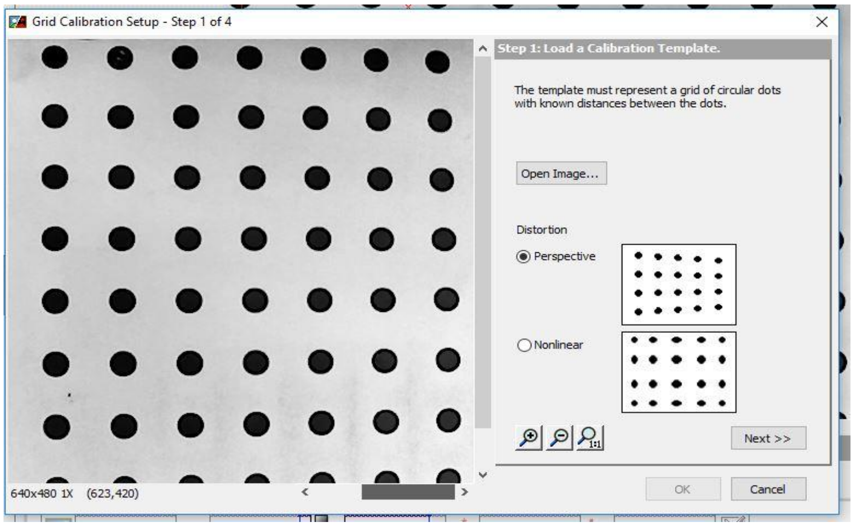

Figure 23: Perspective Calibration

Thresholding

- Done for darker region of interest
- Min 0 to Max 128

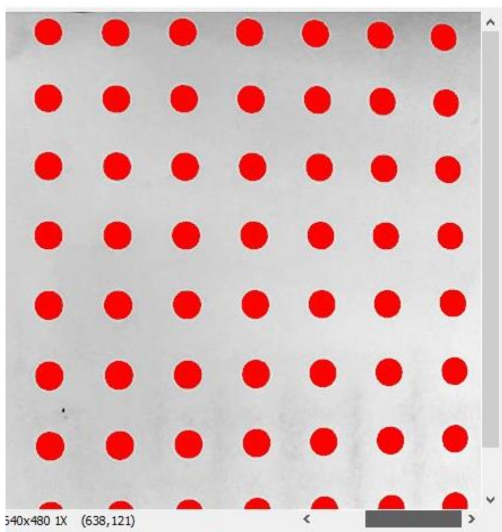

Figure 24: Thresholding

Real World Mapping

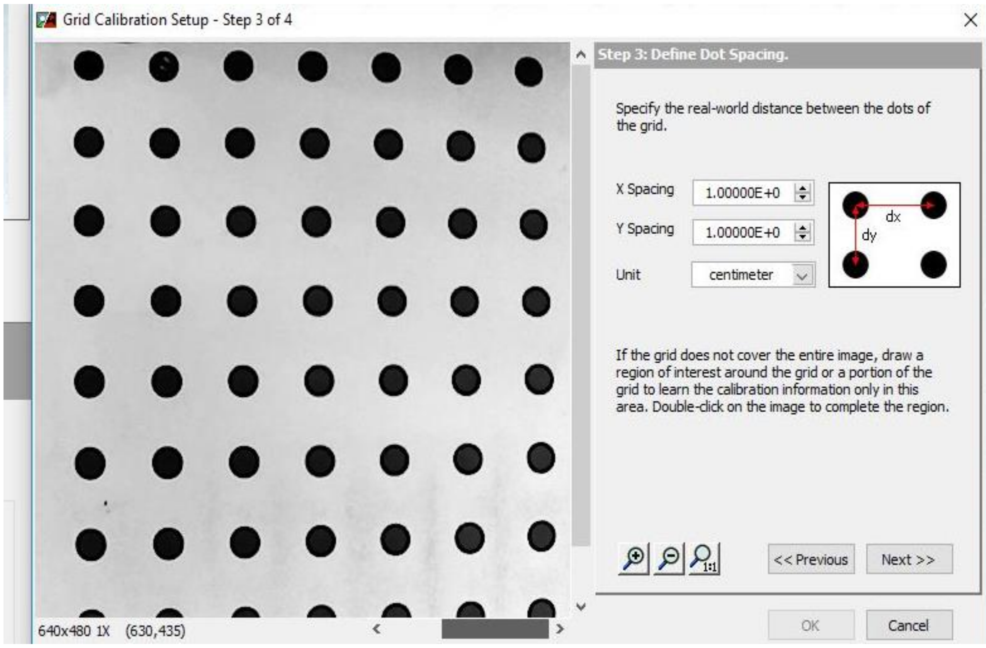

Figure 25: Real World Mapping

- Specify distance between dots
- Specify unit conversion

Calibration Axis

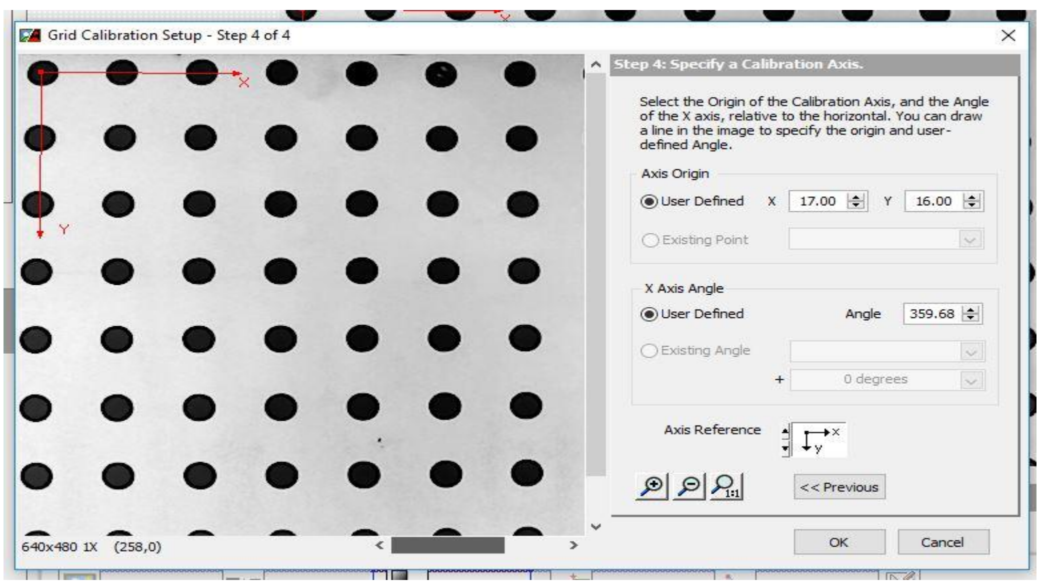

Figure 26: Calibration Axis

- Axis mapping
- Origin is defined in real world
- Axis Reference was also set accordingly

<u>Edge Detection</u>

- In machine vision edge detection was chosen to know whether designed system has learnt grid calibration for all the points or not
- To check that whether designed system reads transitions or not for measurements

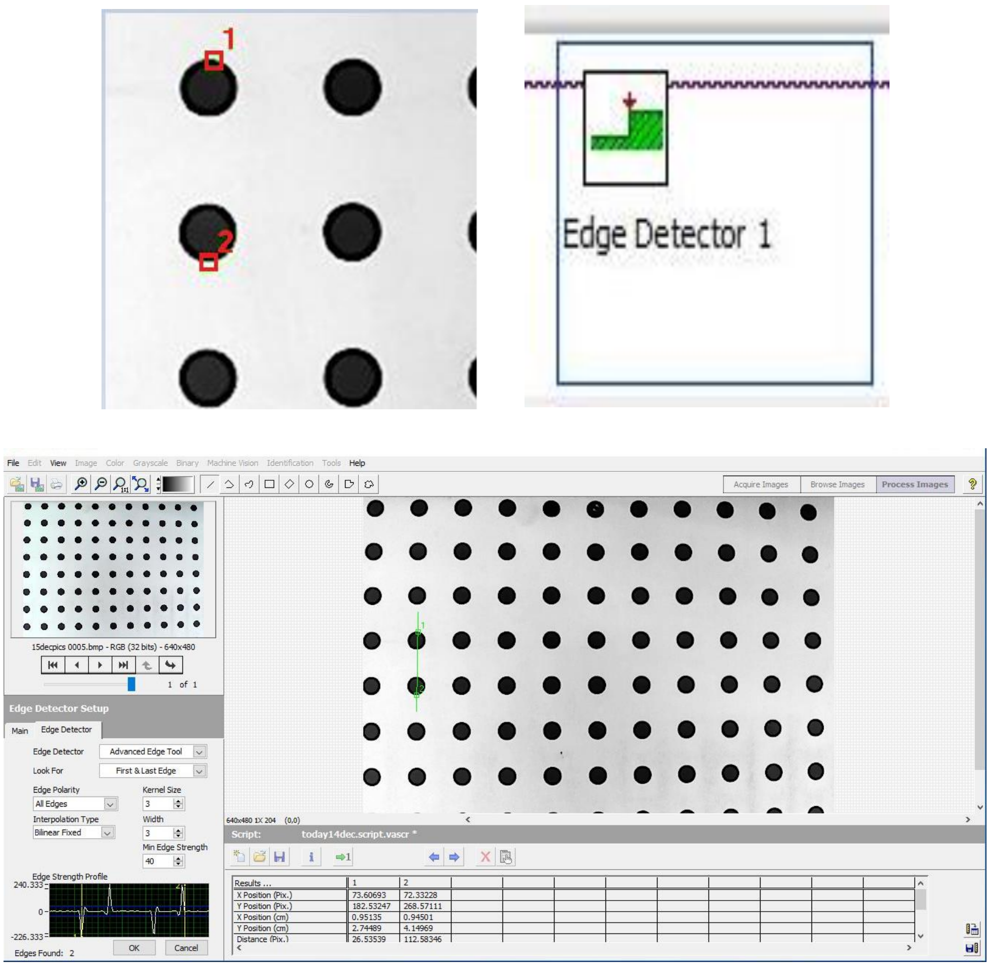

Figure 27: Edge Detection (using points 1 and 2)

Caliper

- Caliper can be used to measure point to point, or edge to edge. Caliper can be configured to measure features horizontally or vertically in the image. It uses advanced edge detection and filtering to locate the two points in a user defined region of interest
- In order to find exact measurements of distance caliper is used
- For defining distance by selecting points 1 and 2 defined by edge detector

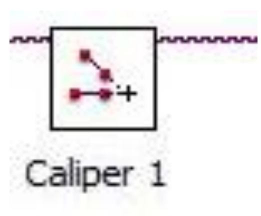

Figure 28: Caliper

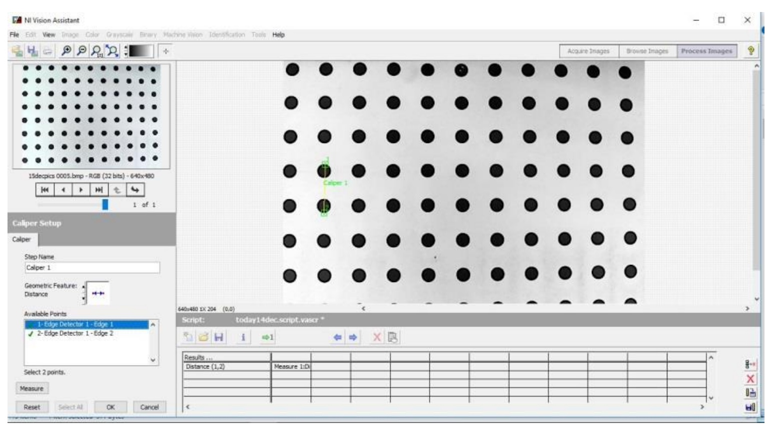

Figure 29 Caliper measurements

Caliper Measurements

This is because it was taken from start of point 1 to the end of point 2 i.e. rising edge of point 1 and falling edge of point 2 that's the reason distance to be measured was 140mm.

Coordinate Transformation

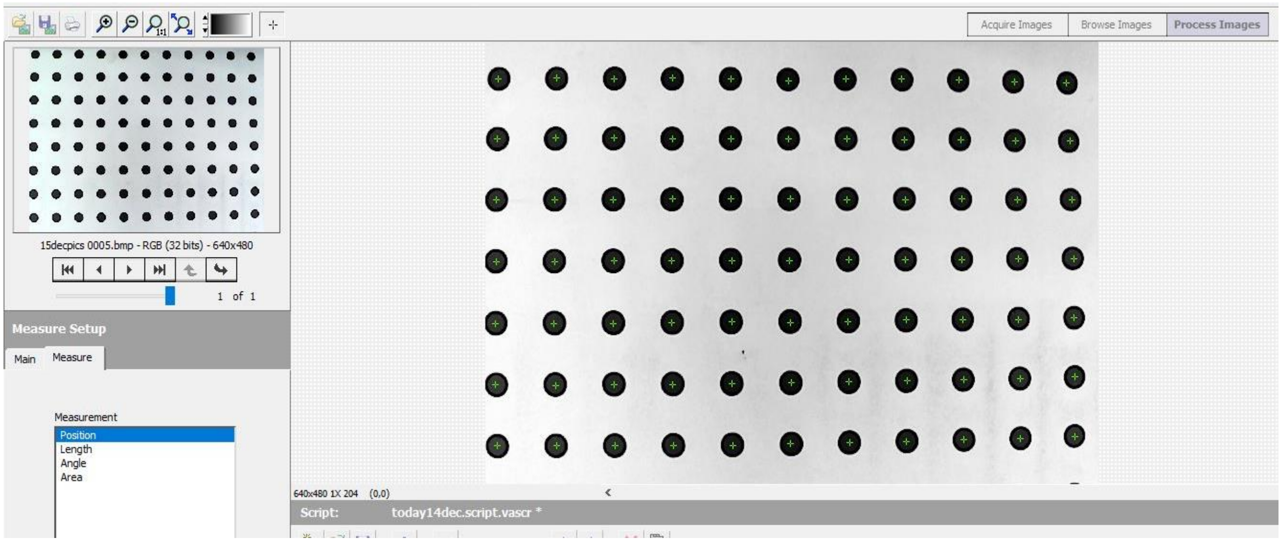

Figure 30: Coordinate Transformation

- Position of each point was mapped from image pixels to real world coordinate system.
- 88 points were chosen from grid calibration for mapping from image coordinates to real world coordinates.
- Results of Mapping X Pos. are shown in chapter 4 of results along with graph
- Results of Mapping Y Pos. are shown in chapter 4 of results along with graph

3.6.3.3 Step 3 Post Processing

Distance Measurement

<u>X-axis distance measurement</u>

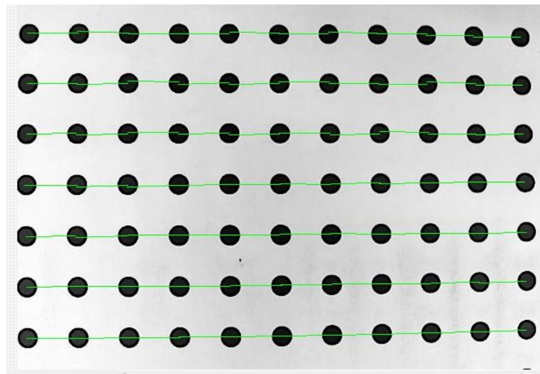

Figure 31: Distance Measurement X-axis

<u>Y-axis distance measurement</u>

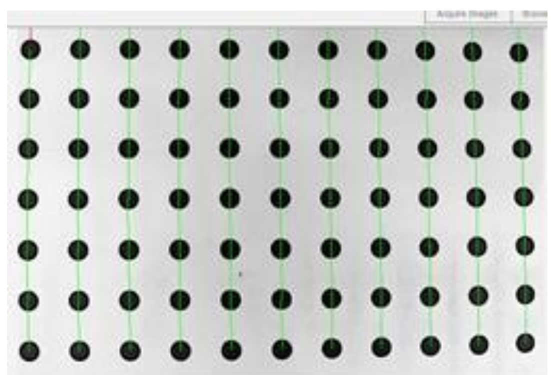

Figure 32: Y-axis distance measurement

Summary Table of Distance Measurement along Y-axis and X-axis are discussed in chapter 4

Y-axis and X-axis distance measurement Graph are also discussed in chapter 4

Angles

1. 90° angle

Summary table of 90 degrees angle is discussed in chapter 4. Graph of 90 degrees is also discussed in chapter 4 this graph shows deviation from 90 degrees

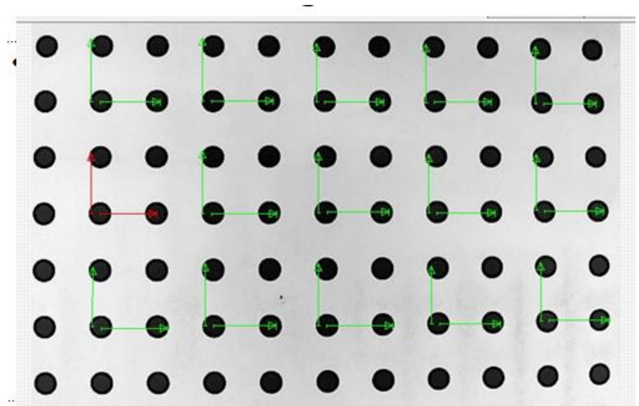

Figure 33: 90° angles

2. 180° Angle measurement

Summary table of 180 degrees is discussed in chapter 4.Graph of 180 degrees is discussed in chapter 4 that graph gives deviation from 180 degrees

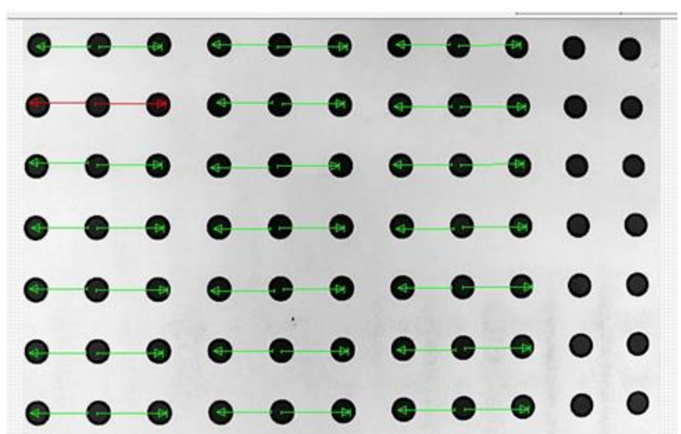

Figure 34: 180° Angle measurements

3. 270 ° angle measurement

Summary table of 270 degrees angle is discussed in chapter 4 .Graph of 270 degrees angle is discussed in chapter 4 that graph shows deviation from 270°

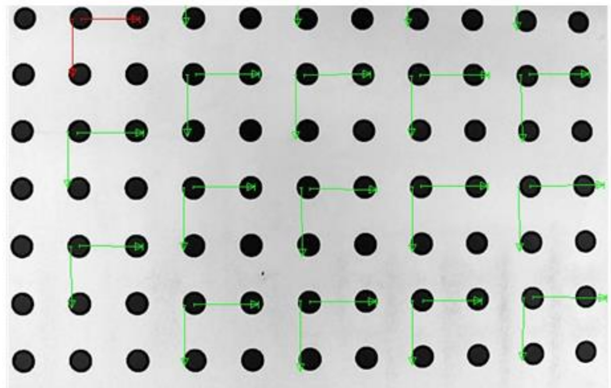

Figure 35: 270 ° angle measurements

3.1.19 Performance meter

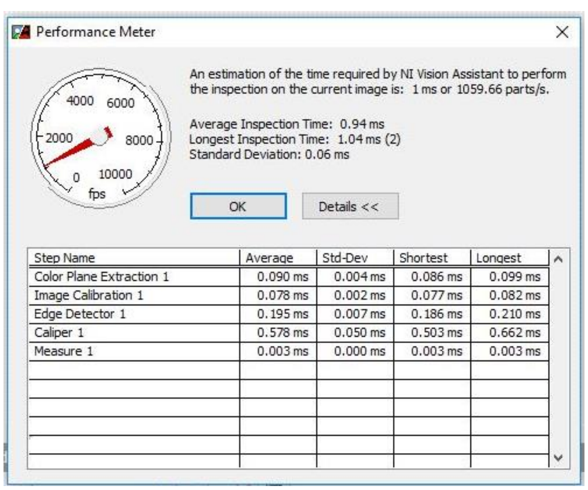

Figure 36: Performance meter

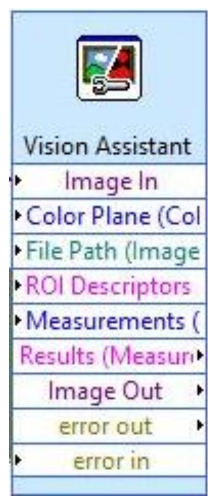

Figure 37: Vision Assistant

It was all done using LabVIEW Assistant

Chapter 4 Results

4.1 Tracking Results:

ROI can be selected via mouse clicking first rectangular box to be selected for tracking drill was First at 289 X axis and 322 at Y axis on coordinates of pixel and it ended at 297 and Y axis 345 on coordinates of pixel. This selected rectangle has length 23 pixels and width 8pixels.

Following picture is showing the results

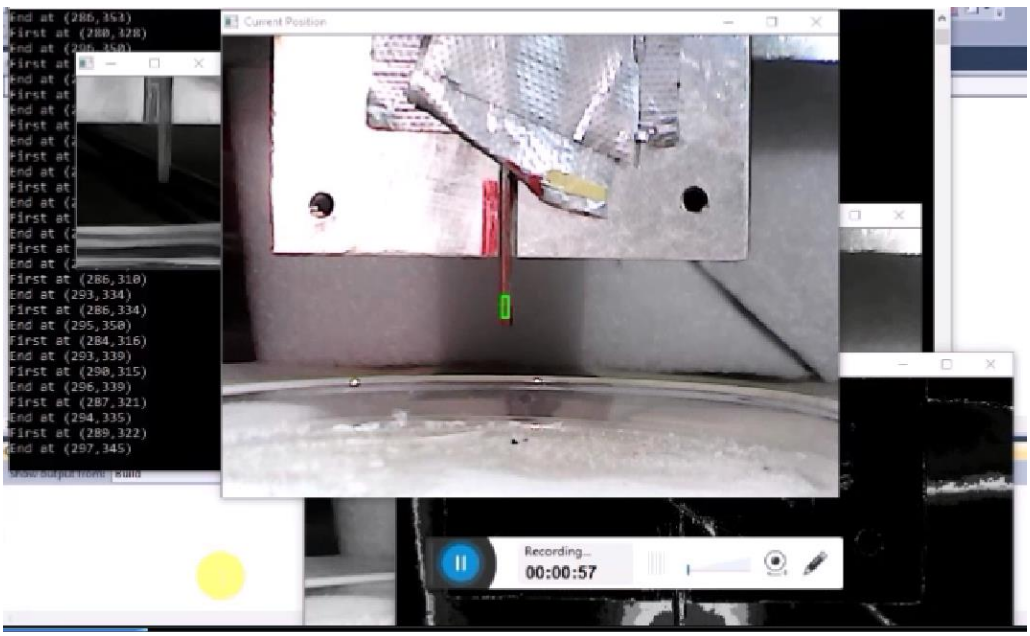

Figure 38: Mean shift Tracking: rectangular ROI was chosen for drill bit of 1.96mm

First at 289 X axis and 322 at Y axis on coordinates of pixel and it ended at 297 and Y axis 345 on coordinates of pixel. This selected rectangle has length 23 pixels and width 8pixels. ROI rectangle for tracking is first at (249, 158) and end at (257,169) coordinates of pixel so it has length 11 pixels and width 8 pixels.

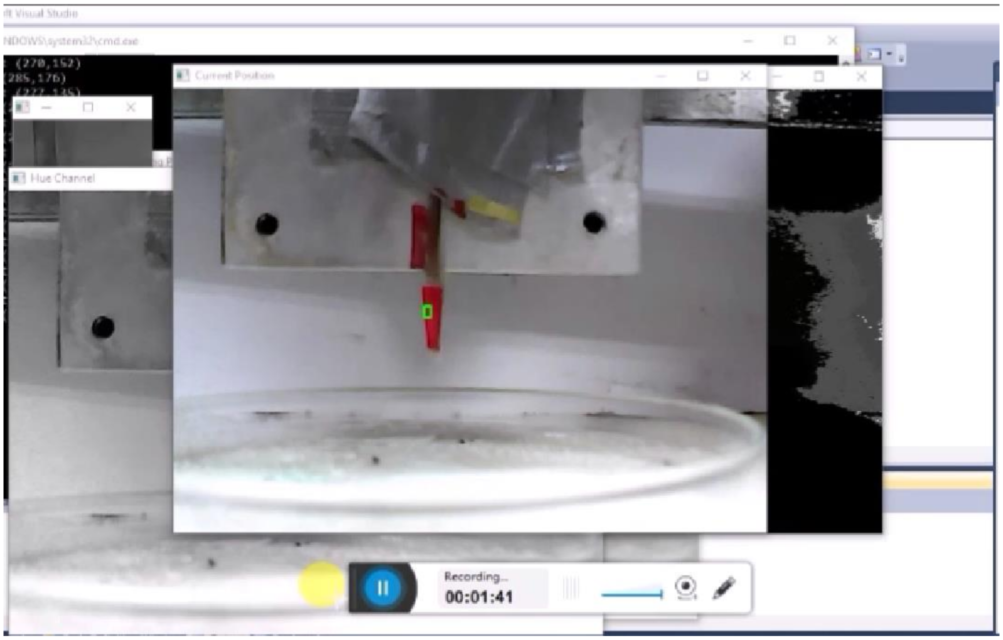

Figure 36: ROI rectangle for tracking was chosen for drill bit of 1.96mm

4.1.1 Hue channel

Figure 37: Mean shift Tracking Hue channel

4.1.2 Back projection

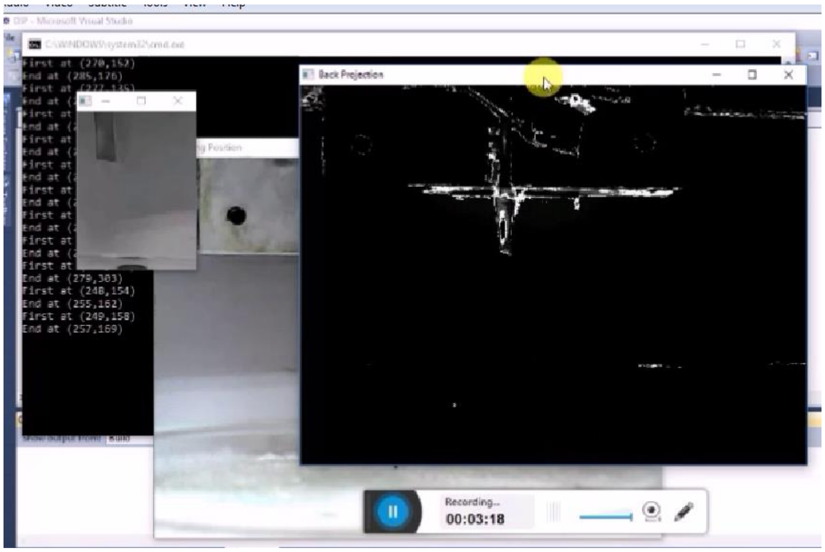

Figure 38: Mean shift Tracking: Back Projection results

4.1.3 Starting position

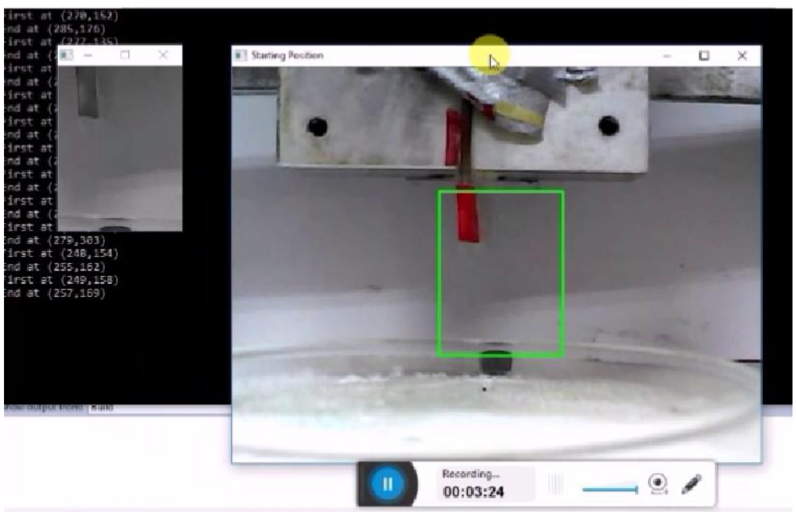

Figure 39: Starting position

4.1.4 ROI selection

For the ROI Selection, command window shows the first and end coordinate points of rectangle as shown in following figure.

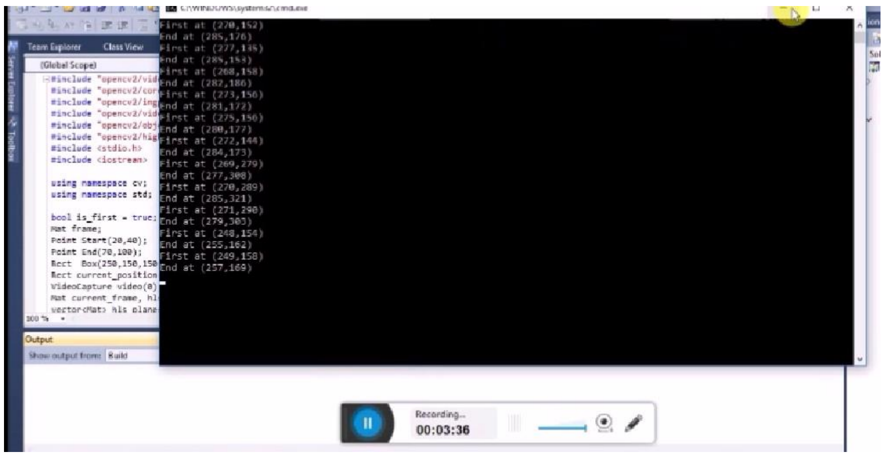

Figure 40: Mean shift Tracking: ROI selection coordinates

The experimental results display that the anticipated method has good presentation in real-time and satisfactory accuracy and precision.

4.1.5 Finding Position coordinates on mouse clicking

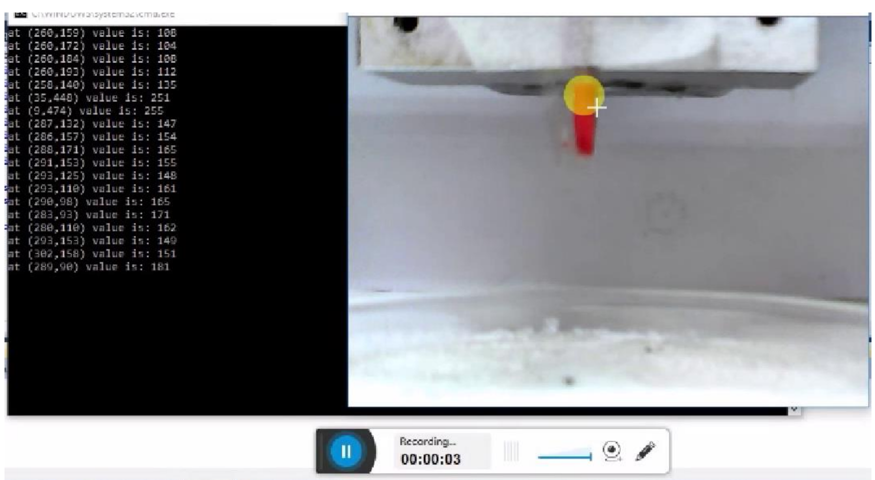

Figure 41: Mean shift Tracking: Results of mouse clicking

To know exactly where drill is actually for finding distance traveled by drill pixel coordinates were found it not only gave pixel coordinates upon clicking but also gave value of pixel value in luminance for red its range was from 150 to 172, this is because luminance channel was chosen at that specific point. Maximum value for luminance is 240 and minimum value for is 0 luminance following figure shows the results as upon clicking red drill bit values from 150 to 172 were observed. It not only gave luminance value it also gave coordinate values in pixel at that specific point from which it can be checked where exactly drill is in video output.

4.1.6 Advantages

Works best in luminance as light does not affect the results

4.1.7 Problems

- Slower as it takes some time to calculate mean to reach at next position
- Single object tracking as mean shift algorithm works only for single object tracking.
- Slowing down the system
- Limitations because of processor
- Real world mapping was not done

4.2 Red Particle filter tracking

4.2.1 Red Particle Filter Tracking Results

It took about average 0.01 seconds to reach red point.

Results

Red particle filter analysis takes time i.e. error correction time to reach red drill as shown in following figure. It works for single object tracking higher and red saturation points or number of pixels.

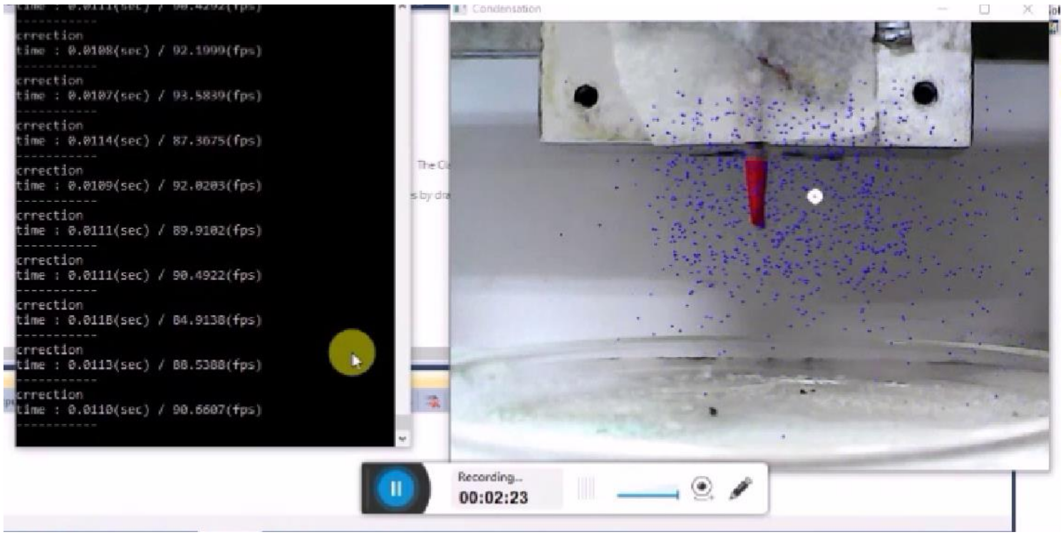

Figure 42: Red Particle Filter Tracking results

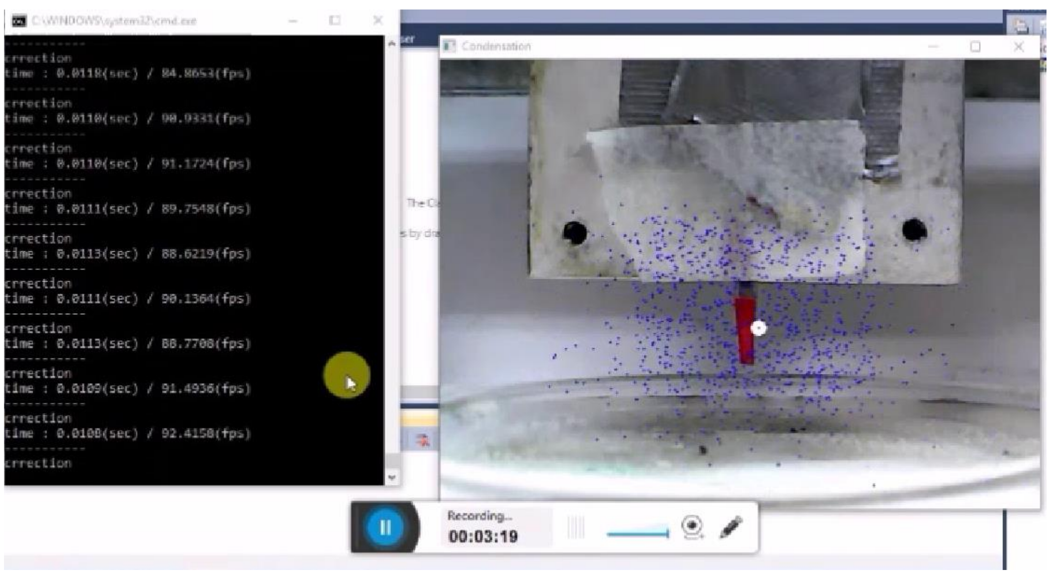

Figure 43: Red Particle filter

It took about average 0.01 seconds to reach red point.

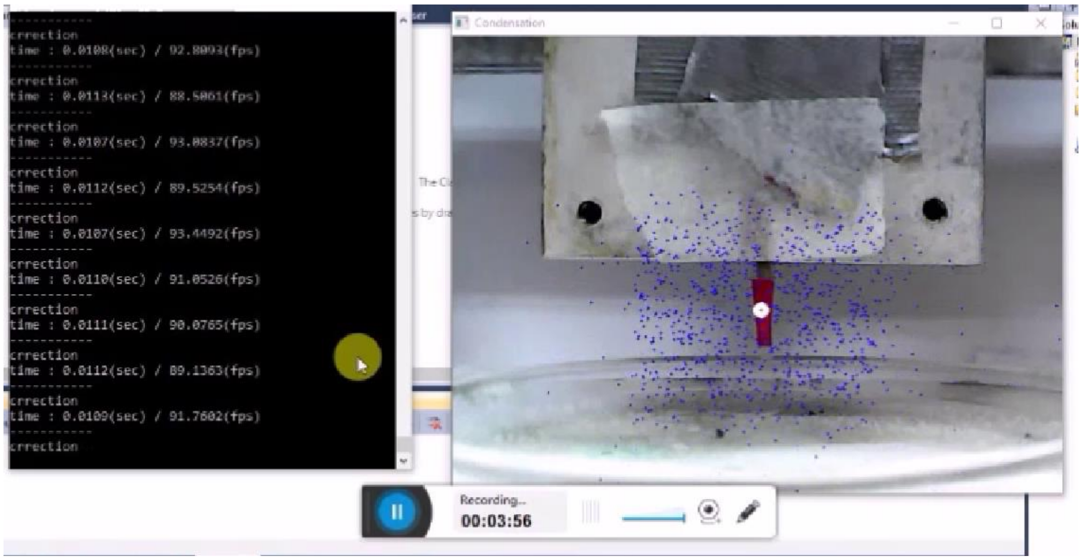

Figure 44: Red Particle Filter results

4.2.2 Works for High saturation

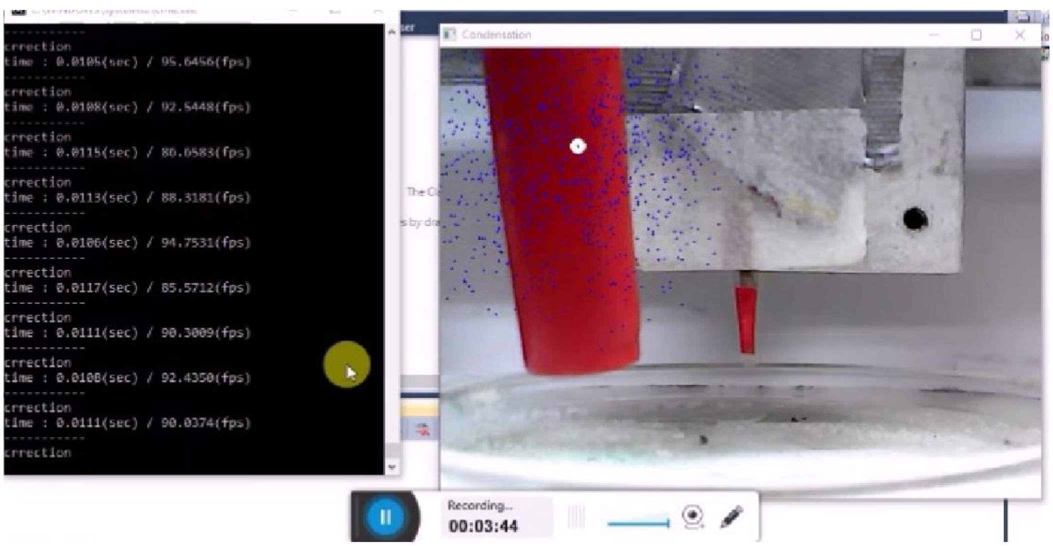

Figure 45: Red Particle Filter results. It prefers higher saturation

4.2.3 Single object tracking

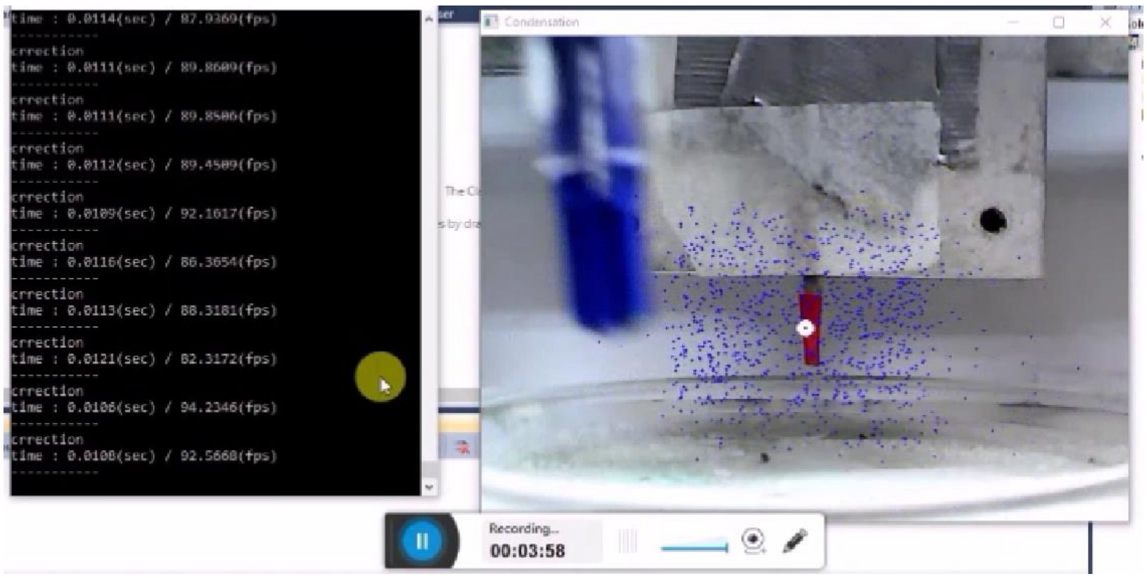

Figure 46: Single object tracking

4.2.4 Problems

- Average error correction time was 0.01 seconds
- Not stable
- Failure occurs because of illumination
- Worked better for higher saturation pixel
- Single object tracking

4.3 NI LabVIEW Vision

4.3.1 Results of Edge Detection

Table 1: Results of Edge Detection

Edge #	X-position (pix.)	Y-position(pix.)	X-position(mm)	Y-position(mm)	Distance(pixel)	Distance(mm)	Rising
1	73.60693	182.53247	9.5135	27.4489	26.53539	4.3604	0
2	72.33228	268.57111	9.4501	41.4969	112.58346	18.4086	1

4.3.2 Results of Caliper

Table 2: Result of Caliper

Step Type	Result Name	Value	Unit
Caliper	Distance in pixels	86.05	pixels
Caliper	Distance in Real World	140	mm

This is because it was taken from start of point 1 to the end of point 2 i.e. rising edge of point 1 and falling edge of point 2 that's the reason distance to be measured was 140mm.

4.3.3 Results of Mapping X Pos.

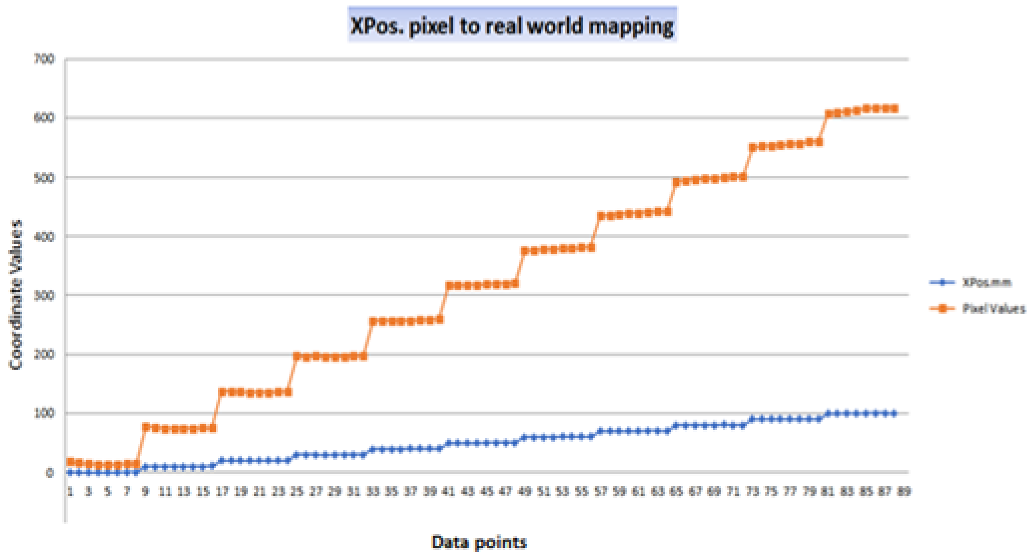

Figure 47: Results of Mapping X Pos.

4.3.4 Results of Mapping Y Pos.

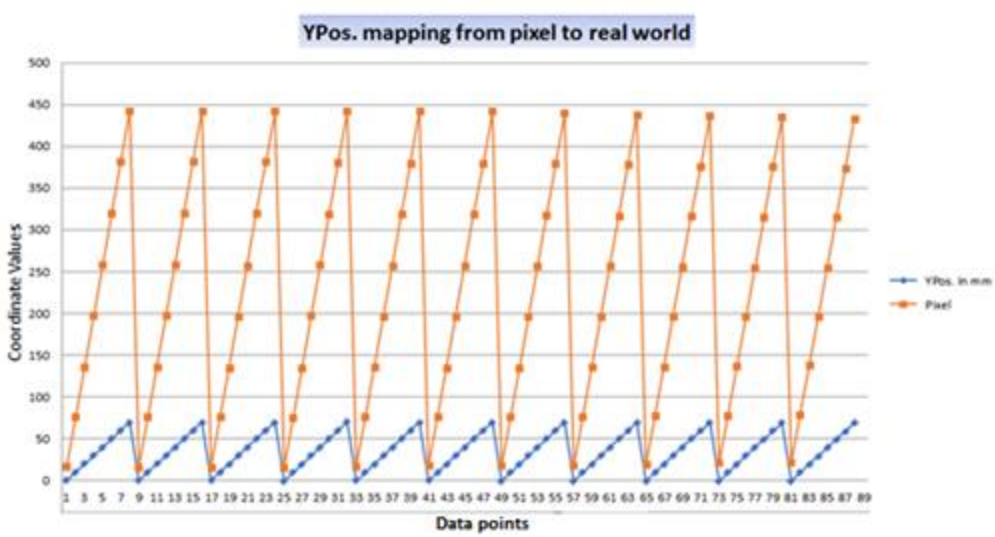

Figure 48: Results of Mapping Y Pos.

4.3.5 Distance measurement

4.3.5.1 Summary table of X-axis measurement

Table 3: Summary Table of distance measurement along X-axis

Valid N	Mean (mm)	STD-Dev (mm)
80	10.147	0.1886

4.3.5.2 Graph X-axis distance measurement

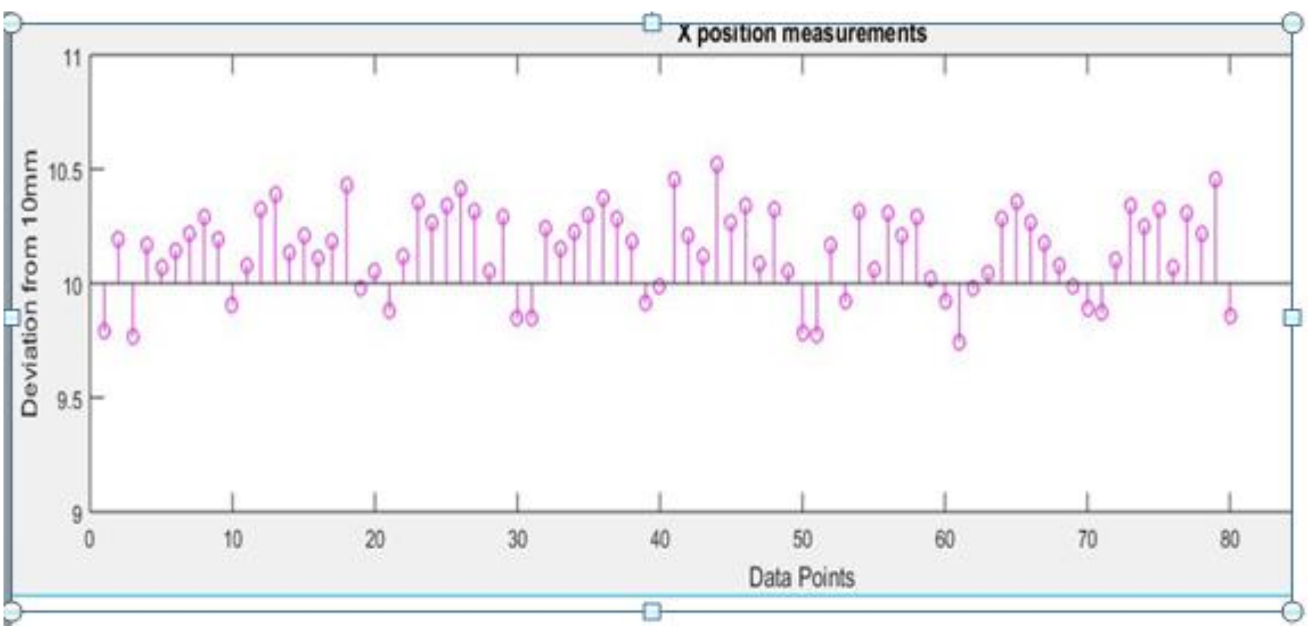

Figure 49: Graph X-axis distance measurement

Y-axis distance measurement

4.3.5.3 Summary Table of Distance Measurement along Y-axis

Table 4: Summary Table of Distance Measurement along Y-axis

Variable	Valid N	Mean(mm)	Std. Dev(mm)
Length measurement Along Y-axis	77	10.09473	0.1744

4.3.5.4 Y-axis distance measurement Graph

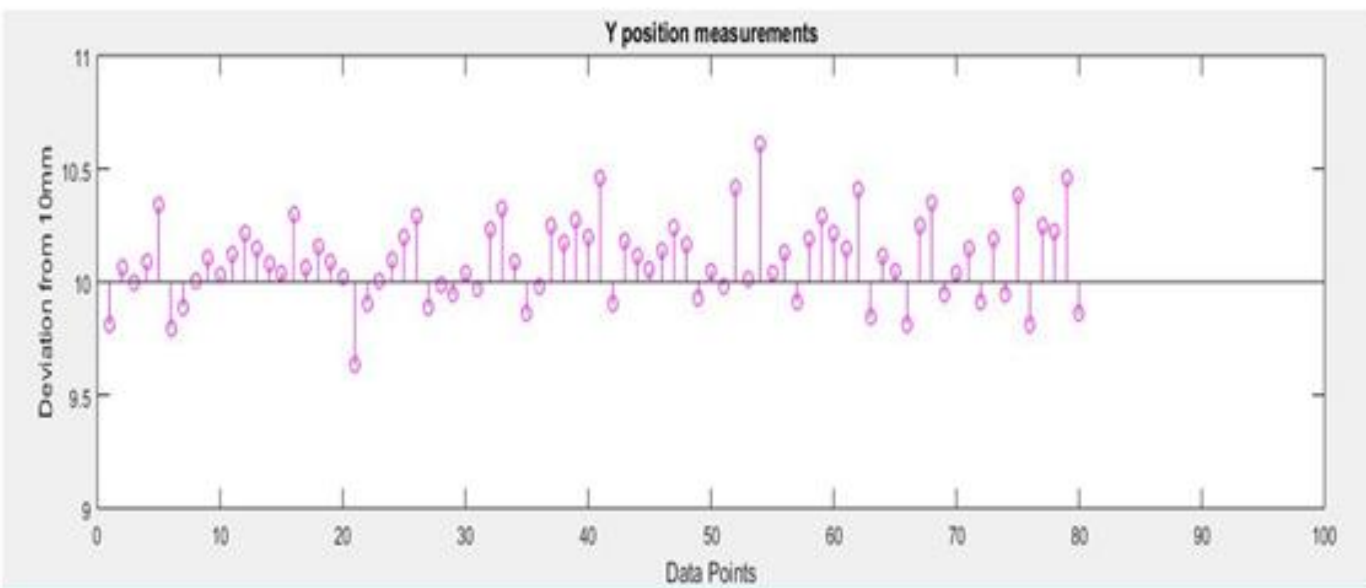

Figure 50: Y-axis distance measurement Graph

4.3.6 Angles measurement

4.3.6.1 90 ° angle measurement

<u>Summary table of 90 degrees angle</u>

Table 5: Summary table of 90 degrees angle

Variable	Valid N	Mean	Std. Dev.
Angle measurement	24	89.94°	0.227°

<u>Graph of 90 degrees</u>

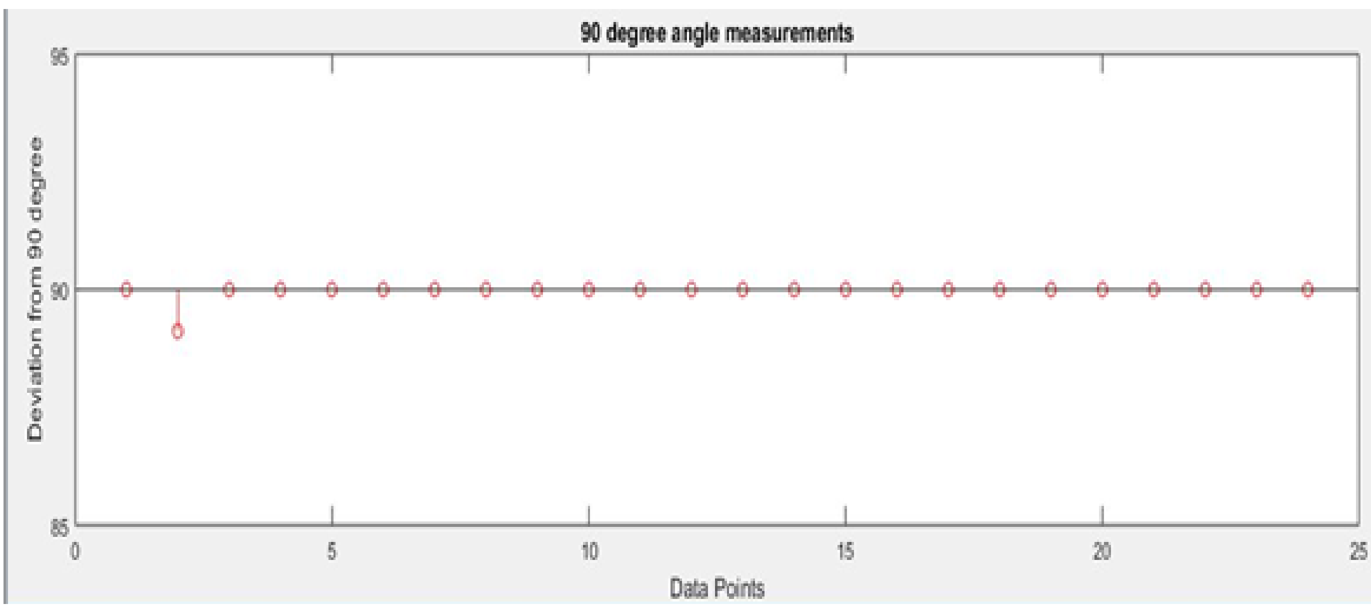

Figure 51: This graph shows deviation from 90 degrees

4.3.6.2 180° Angle measurement

Summary table of 180 degrees

Table 6: Summary table of 180 degrees

Variable	Valid N	Mean(degrees)	Std. Dev.
Angle measurement	24	179.92°	0.258°

Graph of 180 degrees

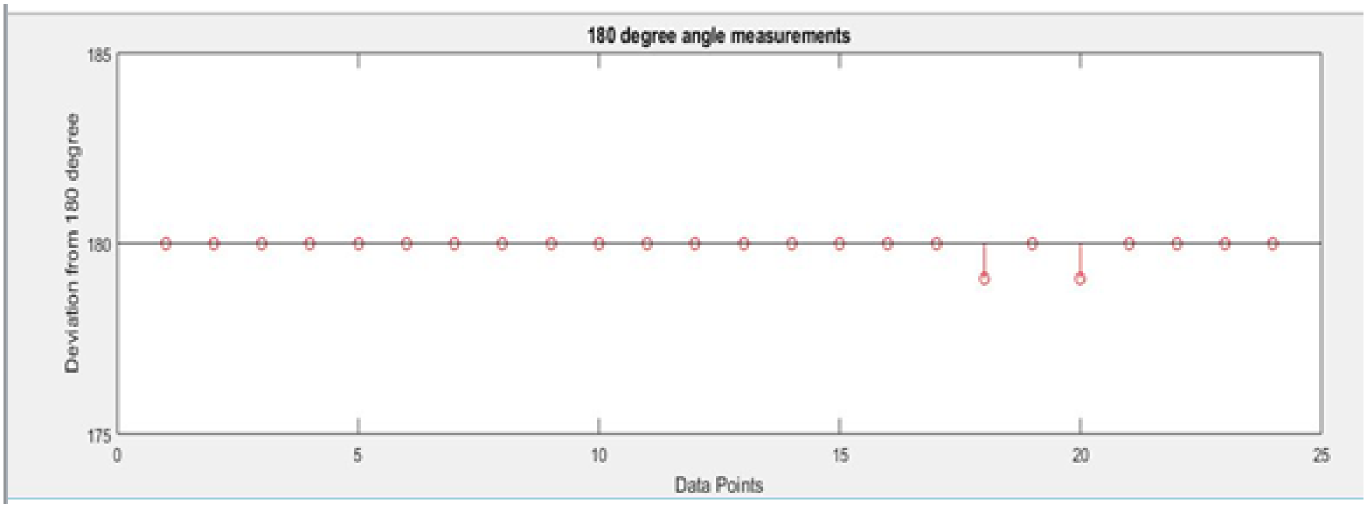

Figure 52: This graph gives deviation from 180 degrees

4.3.6.3 Graph of 270 degrees

Summary table of 270 degrees angle

Table 7: Summary table of 270 degrees angle

Variable	Valid N	Mean(degrees)	Std. Dev.
Angle measurement	24	270.2558°	0.667°

Graph of 270° degrees angle

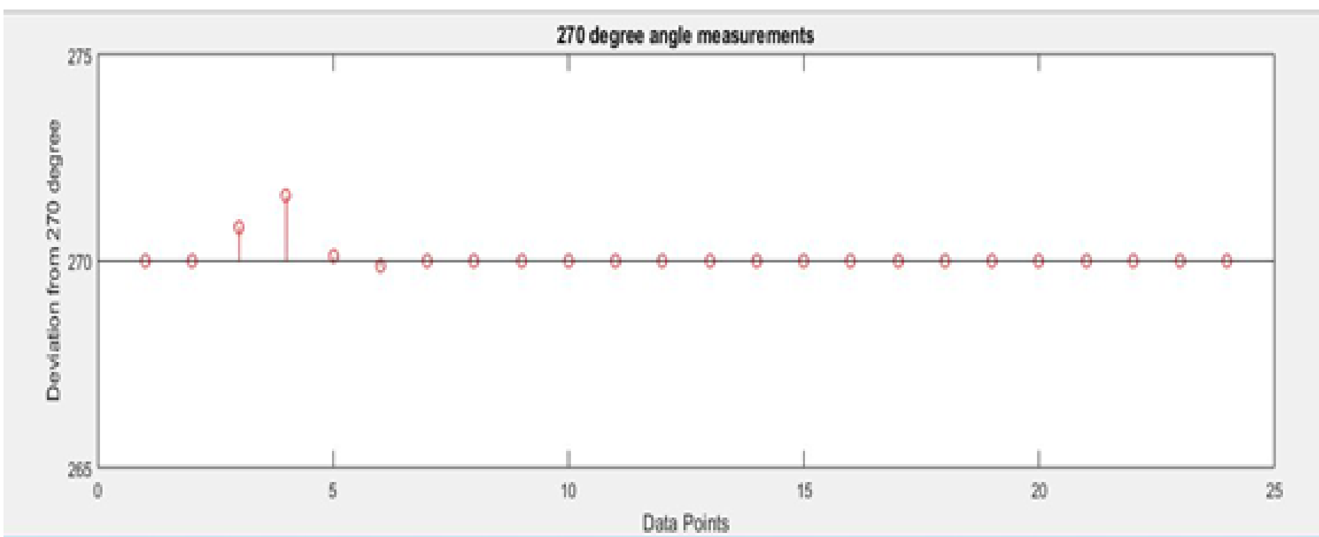

Figure 53: This graph shows deviation from 270°

4.3.6.4 Performance meter

Table 8: Performance meter

Step name	Avg.	Standard deviation	shortest	longest
Color plane extraction	0.090ms	0.004ms	0.086ms	0.099ms
Image calibration	0.078ms	0.002ms	0.077ms	0.082ms
Edge detector	0.195ms	0.007ms	0.186ms	0.210ms
Caliper	0.578ms	0.050ms	0.503ms	0.662ms
Measurement	0.003ms	0.000ms	0.003ms	0.003ms

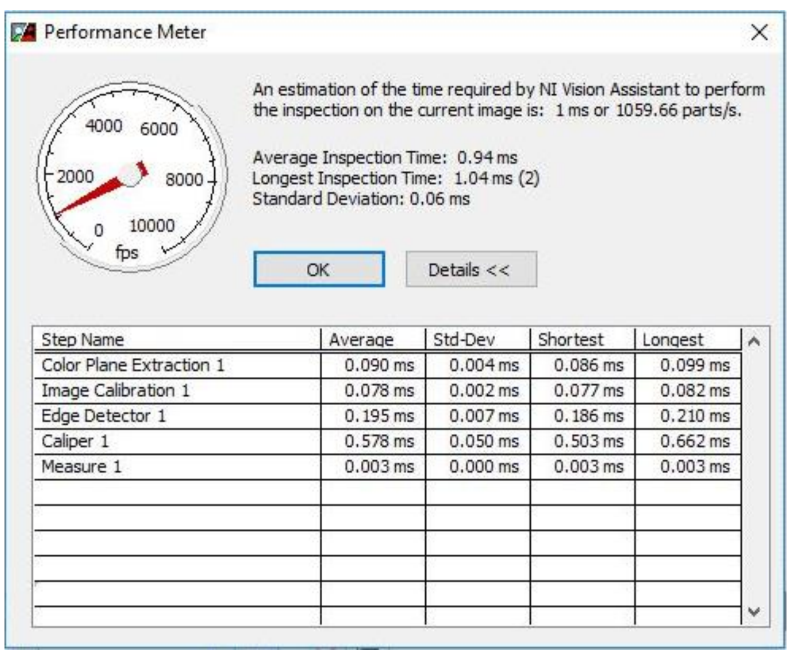

Figure 54: Performance meter

Chapter 5 Discussion of Results

5.1 Tracking

5.1.1 Results

The experimental results show that the proposed method has good presentation in real-time and satisfactory accuracy, robustness, and positioning precision

To find Position coordinates on mouse clicking and to know exactly where drill is actually so for finding distance traveled by drill, pixel coordinates were found it not only gave pixel coordinates upon clicking but also gave value of pixel value in luminance for red its range was from 150 to 172, this is because luminance channel was chosen at that specific point. Maximum value for luminance is 240 and minimum value for is 0 luminance following figure shows the results as upon clicking red drill bit values from 150 to 172 were observed. It not only gave luminance value it also gave coordinate values in pixel at that specific point from which it can be checked where exactly drill is in video output.

5.1.2 Advantages

- Works best in luminance as light does not affect the results

5.1.3 Problems:

- Slower as it takes some time to calculate mean to reach at next position
- Single object tracking as mean shift algorithm works only for single object tracking.
- Slowing down the system
- Limitations because of processor
- Real world mapping was not done

5.2 Red particle filter analysis

It can cause failure of tracking when the light changes and deformation of the target region occurs. The particle filter shows the probability distribution of the given image with a set of weights so that approximation of the state of the next model is done [19].The weight of the particle is measured by the comparison between the under-consideration image and the target image model.

Finding a consistent and robust feature for target is the key of the particle filter tracking algorithm. Presently, color information (i.e. red color was taken other than this Motion information as well as edge features are the mostly used. The target has good stability which has color distribution and it is not sensitive to the distortion or warp. It can easily be affected by the luminance change and surrounding conditions. To reduce the intrusion of background, the typical color distribution with the value of the weights using kernel window is improved. Secondly, to predict the state use the improved histogram of color.

Equation 3 distance = sqrt (blue * blue + green * green + (255.0 - red) * (255.0 - red))

In calculating likelihood, if input color is close to red, distance becomes smaller. In here, Blue and green color do not play any role but if you set some target color then track the color)

Equation 4 distance = sqrt ((target Blue - b) ^2 + (target green - g) ^2 + (target red-r) ^2)
If you use HSL color model then it is better.

5.3 LabVIEW Vision

5.3.1 Edge detection and Caliper

This is because it was taken from start of point 1 to the end of point 2 i.e. rising edge of point 1 and falling edge of point 2 that’s the reason distance to be measured was 140mm.

Chapter 6 Limitations, Conclusion and Future works

6.1 Limitations

6.1.1 Mean shift tracking

- Slower as it takes some time to calculate mean to reach at next position
- Single object tracking as mean shift algorithm works only for single object tracking.
- Slowing down the system
- Limitations because of processor
- Real world mapping was not done

6.1.2 Particle Filter Tracking

- Average error correction time was 0.01 seconds
- Not stable
- Failure occurs because of illumination
- Worked better for higher saturation pixel
- Single object tracking

6.1.3 LabVIEW Vision

- Optimization problem
- It needs multi -threading and core programming for real time processing system
- To speed up this process, Vision Acquisition hardware is required which is compatible with NI LabVIEW Vision and has inbuilt RT (Real Time) module too.
- It also needs add-ons like VDM, VAS, and Vision express along with NI LabVIEW which makes it cumbersome.

6.2 Conclusion

- Drill tracking in OpenCV was done
- Grid calibration
- Position measurement
- Length measurement
- Angle measurement in LabVIEW was done

6.3 Future works

- Real time system
- 3D systems according to imaging modality
- Superimposition with brain atlas

Chapter 7 References

1. Rickards, H., C. Wood, and A.E. Cavanna, *Hassler and Dieckmann's seminal paper on stereotactic thalamotomy for Gilles de la Tourette syndrome: translation and critical reappraisal.* Movement Disorders, 2008. 23(14): p. 1966-1972.
2. Paxinos, G., et al., *Bregma, lambda and the interaural midpoint in stereotaxic surgery with rats of different sex, strain and weight.* Journal of neuroscience methods, 1985. 13(2): p. 139-143.
3. Solf, T. and K. Eck, *Method of and imaging ultrasound system for determining the position of a catheter*, 2003, Google Patents.
4. Kwoh, Y.S., et al., *A robot with improved absolute positioning accuracy for CT guided stereotactic brain surgery.* IEEE Transactions on Biomedical Engineering, 1988. 35(2): p. 153-160.
5. Bucholz, R.D., *System for indicating the position of a surgical probe within a head on an image of the head*, 1995, Google Patents.
6. Unsgaard, G., et al., *Intra-operative 3D ultrasound in neurosurgery.* Acta neurochirurgica, 2006. 148(3): p. 235-253.
7. Gibon, D., et al., *Stereotactic localization in medical imaging: A technical and methodological review.* Journal of Radiosurgery, 1999. 2(3): p. 167-180.
8. Kuhl, C.K., et al., *Interventional breast MR imaging: clinical use of a stereotactic localization and biopsy device.* Radiology, 1997. 204(3): p. 667-675.
9. Masura, J., et al., *Catheter closure of moderate-to large-sized patent ductus arteriosus using the new Amplatzer duct occluder: immediate and short-term results.* Journal of the American College of Cardiology, 1998. 31(4): p. 878-882.
10. Shmulewitz, A. and E. Ziring, *Image-guided biopsy apparatus with enhanced imaging and methods*, 1997, Google Patents.
11. Wisner, K., et al., *Ratat1: a digital rat brain stereotaxic atlas derived from high-resolution MRI images scanned in three dimensions.* Frontiers in systems neuroscience, 2016. 10: p. 64.
12. Aggarwal, M., et al., *Magnetic resonance imaging and micro-computed tomography combined atlas of developing and adult mouse brains for stereotaxic surgery.* Neuroscience, 2009. 162(4): p. 1339-1350.
13. Pak, N., et al., *Closed-loop, ultraprecise, automated craniotomies.* Journal of neurophysiology, 2015. 113(10): p. 3943-3953.
14. Rousseau, J., et al., *A frameless method for 3D MRI-and CT guided stereotaxic localisation.* European Radiology, 1992. 2(1): p. 35-41.
15. Ji, S., et al. *An integrated model-based neurosurgical guidance system*. in *Medical Imaging 2010: Visualization, Image-Guided Procedures, and Modeling*. 2010. International Society for Optics and Photonics.
16. Robb, R.A., et al., *Analyze: a comprehensive, operator-interactive software package for multidimensional medical image display and analysis.* Computerized Medical Imaging and Graphics, 1989. 13(6): p. 433-454.
17. Allen, G.S., et al., *Interactive image-guided surgical system*, 1992, Google Patents.

18. Assmann, S., *ARRANGEMENT FOR MONITORING A POSITIONING OF A PROSTHETIC CARDIAC VALVE AND CORRESPONDING METHOD*, 2017, US Patent App. 15/603,594.
19. Comaniciu, D., V. Ramesh, and P. Meer, *Kernel-based object tracking.* IEEE Transactions on Pattern Analysis and Machine Intelligence, 2003. 25(5): p. 564-577.
20. Lehn-Schiøler, T., Erdogmus, D., Principe, J.C.: Parzen Particle Filters. In: ICASSP 2004, vol. 5, pp. 781–784 (2004)
21. *Particle Filter Based Object Tracking in Video* Swati S. Jadhav, Rohita P. PatilISSN: 2278 – 909X International Journal of Advanced Research in Electronics and Communication Engineering (IJARECE) Volume 5, Issue 6, June 2016
22. *Object Tracking Based on Parzen Particle Filter Using Multiple Cues*
Lei Song, Rong Zhang, Zhengkai Liu, and Xingxing Chen MOE-Microsoft Key laboratory of Multimedia Computing and Communication Department of Electronic Engineering and Information Science University of Science and Technology of China 230027HeFei,P.R.ChinaBakker,R.,Tiesinga,P.,andKotter,R.(2015).Thescalablebrainatlas: instantwebbased access to public brain atlases and related content. Neuroinformatics 13, 353–366.doi:10.1007/s12021-014-9258-x Calabrese, E., Johnson, G. A., and Watson, C. (2013).
23. *An ontology-based segmentation scheme for tracking postnatal changes in the developing rodent brain with MRI.* Neuroimage 67, 375–384. doi: 10.1016/j.neuroimage. 2012.11.037 Odintsov, B. (2011). Tunable Radio-Frequency Coil.
24. USAPatent Application 61081954.Washington,DC:UnitedStatesPatentandTrademarkOffice. Papp,E.A.,Leergaard,T.B.,Calabrese,E.,Johnson,G.A.,andBjaalie,J.G.(2014). WaxholmSpaceatlasoftheSpragueDawleyratbrain.Neuroimage97,374–386. doi:10.1016/j.neuroimage.2014.04.001 *Paxinos, G., and Watson*, C. (1998).
25. *The Rat Brain in Stereotaxic Coordinates*. NewYork,NY:AcademicPress. Schweinhardt, P., Fransson, P., Olson, L., Spenger, C., and Andersson, J. L. (2003). A template for spatial normalisation of MR images of the rat
26. brain. J. Neurosci. Methods 129, 105–113. doi: 10.1016/S0165-0270(03)00 192-4 Valdes-Hernandez,P.A.,Sumiyoshi,A.,Nonaka,H.,Haga,R.,Aubert-Vasquez,E., Ogawa, T., et al. (2011). *An in vivo MRI template set for morphometry, tissue segmentation, and fMRI localization in rats. Front*. Neuroinform. 5:26. doi: 10.3389/fninf.2011.00026
Allen Mouse Brain Atlas [Internet]: Allen Institute for Brain Science. http://mouse.brain-map.org.
27. Lafitte, F., Boukobza, M., Guichard, J. P., Hoeffel, C., Reizine, D., Ille, O., ... & Merland, J. J. (1997). *MRI and MRA for diagnosis and follow-up of cerebral venous thrombosis* (CVT). Clinical radiology, 52(9), 672-
28. 679.
29. Shung, K. K. (2009). *High frequency ultrasonic imaging. Journal of medical ultrasound*, 17(1), 25-30.
30. [3] Unsgaard, G., Ommedal, S., Muller, T., Gronningsaeter, A., & Hernes, T. A. N. (2002). *Neuronavigation by intraoperative three-dimensional ultrasound: initial experience during brain tumor resection. Neurosurgery*, 50(4), 804-812.

31. Hassler, R., & Dieckmann, G. (1969*). Locomotor movements in opposite directions induced by stimulation of pallidum or of putamen*. Journal of the neurological sciences, 8(1), 189-195.
32. Unsgaard, G., Rygh, O. M., Selbekk, T., Müller, T. B., Kolstad, F., Lindseth, F., & Hernes, T. N. (2006). *Intra-operative 3D ultrasound in neurosurgery*. Acta neurochirurgica, 148(3), 235-253.
33. Paxinos, G., Watson, C., Pennisi, M., & Topple, A. (1985). *Bregma, lambda and the interaural midpoint in stereotaxic surgery with rats of different sex, strain and weight. Journal of neuroscience methods*, 13(2), 139-143.
34. Koivukangas, J., Louhisalmi, Y., Alakuijala, J., & Oikarinen, J. (1993). *Ultrasound-controlled neuronavigator-guided brain surgery*. Journal of neurosurgery, 79(1), 36-42.
.
35. Chader, M. D., Faul, I., Feaver, T. L., & Schulz, W. A. (1997). U.S. Patent No. 5,617,857. Washington, DC: U.S. Patent and Trademark Office.
36. Kwoh, Y. S., Hou, J., Jonckheere, E. A., & Hayati, S. (1988). *A robot with improved absolute positioning accuracy for CT guided stereotactic brain surgery*. IEEE Transactions on Biomedical Engineering, 35(2), 153-160.
37. Unsgaard, G., Rygh, O. M., Selbekk, T., Müller, T. B., Kolstad, F., Lindseth, F., & Hernes, T. N. (2006). *Intra-operative 3D ultrasound in neurosurgery*. Acta neurochirurgica, 148(3), 235-253.
38. Kellner, C. H., Jolley, R. R., Holgate, R. C., Austin, L., Lydiard, R. B., Laraia, M., & Ballenger, J. C. (1991). *Brain MRI in obsessive-compulsive disorder*. Psychiatry research, 36(1), 45-49.
39. Larson, P. S., Starr, P. A., Bates, G., Tansey, L., Richardson, R. M., & Martin, A. J. (2012). *An optimized system for interventional MRI guided stereotactic surgery: preliminary evaluation of targeting accuracy*. Neurosurgery, 70(OPERATIVE), ons95.
40. Kelly, P. J., & Goerss, S. J. (1996). U.S. Patent No. 5,483,961. Washington, DC: U.S. Patent and Trademark Office.
41. Hata, N., Dohi, T., Iseki, H., & Takakura, K. (1997). *Development of a frameless and armless stereotactic neuronavigation system with ultrasonographic registration. Neurosurgery*, 41(3), 608-614.
42. Barnett, G. H., Kormos, D. W., Steiner, C. P., & Weisenberger, J. R. (1993). *Use of a Frameless, Armless Stereotactic Wand for Brain Tumor Localization with Two-Dimensional and Three-Dimensional Neuroimaging. Neurosurgery*, 33(4), 674-678.
43. Saad, S. A. (1998). U.S. Patent No. 5,727,553. Washington, DC: U.S. Patent and Trademark Office.
44. Glowinski, A., & Van Vaals, J. J. (1999). U.S. Patent No. 5,868,674. Washington, DC: U.S. Patent and Trademark Office.
45. Kondziolka, D., Dempsey, P. K., Lunsford, L. D., Kestle, J. R., Dolan, E. J., Kanal, E., & Tasker, R. R. (1992). *A comparison between magnetic resonance imaging and computed tomography for stereotactic coordinate determination. Neurosurgery*, 30(3), 402-407.
46. Govari, A. (2001). *Miniaturized position sensor having photolithographic coils for tracking a medical probe*.

47. Sastry, R., Bi, W. L., Pieper, S., Frisken, S., Kapur, T., Wells, W., & Golby, A. J. (2016). *Applications of Ultrasound in the Resection of Brain Tumors. Journal of Neuroimaging*.
48. Saad, S. A. (1998). U.S. Patent No. 5,727,553. Washington, DC: U.S. Patent and Trademark Office.
49. Glowinski, A., & Van Vaals, J. J. (1999). U.S. Patent No. 5,868,674. Washington, DC: U.S. Patent and Trademark Office.
50. Kelly, P. J., & Goerss, S. J. (1996). U.S. Patent No. 5,483,961. Washington, DC: U.S. Patent and Trademark Office.
51. Kwoh, Y. S., Hou, J., Jonckheere, E. A., & Hayati, S. (1988). *A robot with improved absolute positioning accuracy for CT guided stereotactic brain surgery. IEEE Transactions on Biomedical Engineering*, 35(2), 153-160.
52. *Ratat1*: *A Digital Rat Brain Stereotaxic Atlas Derived from High-Resolution MRI Images Scanned in Three Dimensions* Kurt Wisner1*, Boris Odintsov2
53. *Closed-loop, ultraprecise, automated craniotomies*
Nikita Pak, 1, 2 Joshua H. Siegle, 3* Justin P. Kinney, 1* Daniel J.Denman,3 Timothy J. Blanche
55 Jayesh, H.K., Petar, M.D.: *Gaussian Sum Particle Filtering. IEEE Transactions on Signal Processing* 51(10), 2602–2612 (2003)

Proposed Certificate for Plagiarism

It is certified that PhD/M.Phil. /MS Thesis Titled Image Guided Stereotaxic Surgery System by Namra Afzal NUST-MSBME-000000118246F has been examined by us. We undertake the follows:

a. Thesis has significant new work/knowledge as compared already published or are under consideration to be published elsewhere. No sentence, equation, diagram, table, paragraph or section has been copied verbatim from previous work unless it is placed under quotation marks and duly referenced.
b. The work presented is original and own work of the author (i.e. there is no plagiarism). No ideas, processes, results or words of others have been presented as Author own work.
c. There is no fabrication of data or results which have been compiled/analyzed.
d. There is no falsification by manipulating research materials, equipment or processes, or changing or omitting data or results such that the research is not accurately represented in the research record.
e. The thesis has been checked using TURNITIN (copy of originality report attached) and found within limits as per HEC plagiarism Policy and instructions issued from time to time.

Name & Signature of Supervisor

Dr. Muhammad Nabeel Anwar

Signature: ________________

today 7feb

ORIGINALITY REPORT

11%	4%	8%	4%
SIMILARITY INDEX	INTERNET SOURCES	PUBLICATIONS	STUDENT PAPERS

PRIMARY SOURCES

1	Ji, Songbai, Xiaoyao Fan, Kathryn Fontaine, Alex Hartov, David Roberts, Keith Paulsen, and Michael I. Miga. "", Medical Imaging 2010 Visualization Image-Guided Procedures and Modeling, 2010. Publication	2%
2	Dongsheng Ding, Zengru Jiang, Chengyuan Liu. "Object tracking algorithm based on particle filter with color and texture feature", 2016 35th Chinese Control Conference (CCC), 2016 Publication	1%
3	Pak, Nikita, Joshua H. Siegle, Justin P. Kinney, Daniel J. Denman, Timothy J. Blanche, and Edward S. Boyden. "Closed-loop, ultraprecise, automated craniotomies", Journal of Neurophysiology, 2015. Publication	1%
4	www.ni.com Internet Source	1%

5	Submitted to General Sir John Kotelawala Defence University Student Paper	1%
6	www.science.gov Internet Source	<1%
7	92trade.com Internet Source	<1%
8	spie.org Internet Source	<1%
9	"Abstract Selection", The Journal of Laryngology & Otology, 05/1996 Publication	<1%
10	Submitted to Academic Library Consortium Student Paper	<1%
11	Ching-Shiow Tseng. "Image-guided robotic navigation system for neurosurgery", Journal of Robotic Systems, 08/2000 Publication	<1%
12	Submitted to Newcastle College, Tyne & Wear Student Paper	<1%
13	Haibin Shi, Zhanjian Lin, Weiwei Tang, Bruce Liao, Jolly Wang, Lingxiang Zheng. "Chapter 2 A Robust Hand Tracking Approach Based on Modified Tracking-Learning-Detection Algorithm", Springer Nature, 2014	<1%

Publication

14	www.atsdr.cdc.gov Internet Source	<1%
15	Submitted to University of Westminster Student Paper	<1%
16	Ravi, V.R., A.M.Adil Baig, G. Udhaya Karthick, and S. Thiruchittrambalam. "A Real Time Quality Monitoring System for Engineering Industry: A Practical and Rapid Approach Using Embedded Vision System with LabVIEW", Applied Mechanics and Materials, 2014. Publication	<1%
17	Submitted to University of Newcastle upon Tyne Student Paper	<1%
18	Submitted to University of Strathclyde Student Paper	<1%
19	www.matematicas.uady.mx Internet Source	<1%
20	Submitted to University of Moratuwa Student Paper	<1%
21	Abdul Rahman Hafiz Abdul Ghani. "Bio-Inspired Active Robot Vision Toward Understanding of the Cortical Mechanism", University of Fukui, 2014. Publication	<1%

22	Submitted to City University of Hong Kong Student Paper	<1 %
23	Morokuma, Hidetoshi, Akiyuki Sugiyama, Yasutaka Toyoda, Wataru Nagatomo, Takumichi Sutani, and Ryoichi Matsuoka. "", Metrology Inspection and Process Control for Microlithography XIX, 2005. Publication	<1 %
24	www.ohiolink.edu Internet Source	<1 %
25	etd.lib.metu.edu.tr Internet Source	<1 %
26	Submitted to University of Dayton Student Paper	<1 %
27	flex.flinders.edu.au Internet Source	<1 %

Exclude quotes	Off	Exclude matches	Off
Exclude bibliography	Off		